CHALMERS
UNIVERSITY OF TECHNOLOGY

Thermodynamic and experimental study of the fluoride recovery from Spent Pot Lining recycling process by precipitation of calcium fluoride

Individual project in Chemical Engineering

Anna Mas Herrador

DEPARTMENT OF CHEMISTRY AND CHEMICAL ENGINEERING
CHALMERS UNIVERSITY OF TECHNOLOGY
Gothenburg, Sweden 2020
www.chalmers.se

INDIVIDUAL PROJECT 2020

Thermodynamic and experimental study of the fluoride recovery from Spent Pot Lining recycling process by precipitation of calcium fluoride

ANNA MAS HERRADOR

CHALMERS
UNIVERSITY OF TECHNOLOGY

Department of Chemistry and Chemical Engineering
Division of Nuclear Chemistry and Industrial Materials Recycling
CHALMERS UNIVERSITY OF TECHNOLOGY
Göteborg, Sweden 2020

Thermodynamic and experimental study of the fluoride recovery from Spent Pot Lining recycling process by precipitation of calcium fluoride

Anna Mas Herrador

Supervisor: Burçak Ebin
Individual project 2020
Department of Chemistry and Chemical Engineering
Division of Nuclear Chemistry and Industrial Materials Recycling
Chalmers University of Technology
SE - 412 96 Göteborg
Sweden
Telephone + 46 31 772 1000

Thermodynamic and experimental study of the fluoride recovery from Spent Pot Lining recycling process by precipitation of calcium fluoride

Anna Mas Herrador
Division of Nuclear Chemistry and Industrial Materials Recycling
Department of Chemistry and Chemical Engineering
Chalmers University of Technology

Abstract

The material resulting from removing the electrolytic cell in primary aluminium production is called Spent Pot Lining (SPL). SPL is considered to be toxic due to its high concentration of fluorides and cyanides, corrosive and reactive with water. It is estimated that more than 50% of the SPL generated annually is stored indefinitely or deposited in a landfill. Precipitation is considered a simple and cost-efficient method of removing fluoride from aqueous streams producing a valuable product such as fluorite. In fact, fluorite (CaF_2) is one of 27 critical raw materials for the EU because the risks of supply shortages and their impact on the economy are high. Its high carbon and fluorine content, as well as CaF_2 as the main raw material for almost all fluorochemicals, have made SPL one of the most crucial wastes for recovery, reuse and recycling in a circular economy.

This work is focused on the thermodynamic study to predict the behaviour of a stream coming from an SPL recycling process by introducing calcium salts in order to obtain a precipitated product of interest such as CaF_2, within a circular economy approach. The thermodynamic of the reaction chemistry was investigated by HSC Chemistry software and the subsequent verification of these results in an experimental way.

As a result, the generation of a solid composed of CaF_2 has been verified. Among the three precipitation agents studied, it has been found that the one with higher purity values in thermodynamic calculations is $CaCl_2$ (45.1%). For the real sample, the presence of other precipitates such as Na_2CO_3, CaO, $Ca(OH)_2$, has been observed. A subsequent washing stage is proposed to increase the degree of CaF_2 purity.

Thus, the results present a reliable and environmentally friendly process that produces a product with a high added value. The research indicates that the process could also be applied for the treatment of wastewater with a high concentration of fluorine. The resulting product has a high economic value and could be applied in the aluminium smelting industry.

Keywords: Aluminium production, fluoride recovery, CaF_2 precipitation, thermodynamic modeling

Acknowledgements

This thesis has become a reality with the help of some people and the proper guidance throughout and I would like to extend my gratitude to all of them.

First of all, I would like to thank everyone at the Department of Chemistry and Chemical Engineering, Division of Nuclear Chemistry and Industrial Materials Recycling for making me feel at home from the first days. However, there are some people who deserve special thanks:

My supervisor Burçak Ebin, for all the help, guidance and facilities given to me despite the circumstances during these months of my Erasmus.

My examiner Martina Petranikova, making it possible for me to improve this project.

My colleagues Jonas and Fu for always being willing to help me and not only in the laboratory, as well as Nils and Rasmus, thanks for being more than colleagues.

My office mates, Srija and Mellodee, for sharing good times and laughs.

My Erasmus friends and my great Swedish girl Meli, for filling the pandemic days with joy and adventure.

My family, my siblings and friends from Barcelona, especially Ari and Saray, for supporting me by making the distance disappear. Also to Jose Carlos, for always encouraging me to carry out this experience.

Anna Mas Herrador, Göteborg, July 2020

CONTENTS

LIST OF FIGURES

LIST OF TABLES

1

INTRODUCTION

1.1. Aluminium production

After steel, aluminium is the most highly produced metal and the most produced non-ferrous metal [1]. Worldwide aluminium production in 2019 was approximately 63.7 million tonnes [2]. Due to advances in aluminium alloy metallurgy and also the increase in population and economic activity, these figures are expected to increase.

The primary aluminium production is based on two metallurgical processes: the Bayer process and the Hall-Heroult process. The first process uses bauxite as raw material and the final product is alumina (Al_2O_3). In the electrolytic cells of the Hall-Héroult process, alumina is reduced in a fluorinated bath of cryolite (Na_3AlF_6) under high intensity electrical current. At the bottom of the cells are the carbon cathodes while carbon anodes are held at the top. During the process, the anodes are consumed by reacting with the oxygen released from the alumina input [3,4].

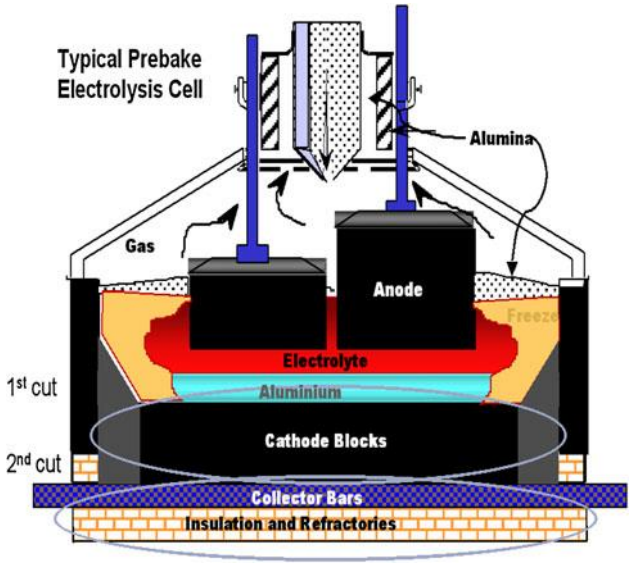

Figure 1 Typical components of a Hall-Héroult cell [5].

Figure 1 shows the components of a Hall-Héroult electrolytic cell. The lining of these cells is built in a steel shell and it is made of carbon. Silicon carbide (SiC) or carbon is used in the side walls. The carbon lining is supported by refractories (fire bricks and insulating bricks). In some cells, calcium silicate boards and steel sheets are present [5].

The electrolysis process consumes most of the energy required for aluminium primary production [4].

Molten aluminium tapped from the electrolysis cells is transported to the cast house where it can be alloyed, cleaned of oxides and gases and then cast into ingots.

Due to the strong reduction conditions, the cell lining wears and can form cracks that reduce its ability to hold the liquid metal in the cell. The pot lining comes to the end of its life after 5-8 years. The life cycle of the cell depends on how it was built, it's design, and its operation [5].

1.2. Spent pot lining

When the failed cell lining is demolished or removed from the electrolytic cell, the shell and lining are demolished. The resulting material is called spent pot lining (SPL).

SPL is typically a mix of all cell lining materials. However, SPL consists of two fractions, as can be seen in Figure 1. The portion above the collector bars is often referred to as the first cut and contains mainly a carbonaceous cathode. It typically consists of a relatively homogeneous and very hard mix of materials including carbon, fluorine and a small amount of cyanide. The first cut forms about 55% of the total weight of the SPL and constitutes the hazardous fraction due to high leachable fluoride and cyanide contents [6].

The fraction below the collector bar or second cut is essentially composed of refractory brick (insulating and firebricks). These insulating materials are used to minimize heat loss through the pot walls. The second cut is typically less homogeneous than the first cut and contains lower levels of cyanide and fluorine. Aluminium, silica and sometimes iron are also present.

There are several factors that contribute to the variability of the SPL composition: initial components for the building of the cell lining depending on the technology used, amount of frozen aluminium that will remain inside the pot depending on the dismantling procedures, operating time, among others.

Also due to the variety of these factors, exact data on the amount of SPL produced are not available. A typical figure would be 22 kg of SPL produced per tonne of aluminium, although it would be between 20 and 50 [6]. In 2018, approximately 1.6 million tonnes of SPL was generated from the production of primary aluminium [7]. Despite improvements in cathode materials may be contributing to a reduction in SPL generation, it is generally recognised that SPL will remain an inevitable waste product of primary aluminium production [8].

It is important to control the downstream process because hazardous SPL by-products can be generated due to the fluoride ion content and cyanide concentration.

Due to the fact that SPL is subjected to high temperatures in aluminium production, water-reactive chemicals are generated. So, SPL is composed of compounds of fluoride, sodium, aluminium, cyanides (caused by the entrance of air through the collector bars), metals (Al, Li and Na), reactive metal oxides (Na_2O), nitrides and carbides. These different compounds will react with moisture to produce NaOH, H_2, C_2H_4, and NH_3 [5].

Thus, SPL is considered a toxic material due to fluoride and cyanide compounds that are leachable in water; corrosive by presenting a high pH due to alkaline metals and oxides; and reactive with water producing flammable, toxic, and explosive gases [5].

Spent Pot Lining is classified as a hazardous waste in several legislations. It is listed in the current EU Waste Catalogue under No. 16 11 01 “Carbon-based linings and refractories from metallurgical processes containing dangerous substances” and No. 16 11 03 “Other linings and refractories from metallurgical processes containing dangerous substances” [7].

It is estimated that more than 50% of the SPL generated annually is stored indefinitely or deposited in a landfill [5]. This can generate problems such as contamination of groundwater and soil, gaseous emissions and biological destruction [6]. Hence, safe removal of SPL requires treatment to stabilize the leachable fluoride and to decompose all compounds of water-reactive and cyanide.

The current practice of landfilling or incineration as waste management of SPL costs aluminium producers an average of 200 EUR/tonne (240 million EUR annually on a global level).

1.3. Circular economy

In the face of the limits of the current linear consumption due to signs of resource depletion, the search for a substantial improvement in resource efficiency throughout the economy is getting louder. The circular economy strategy is proposed to improve energy and resource efficiency and it is based on three principles: waste and pollution removal from design, keeping products and materials in use and regenerating natural systems [9].

Recycling and partial disposal of SPL components have been investigated based on the objectives of this economic model to eliminate waste disposal and incineration costs. Material recirculation with the creation of a high-value chemical also eliminates the need for new raw materials. Therefore, the environmental impact of the aluminium production process is reduced and it contributes to the conservation of resources, also reducing the final disposal of waste.

SPL is an attractive secondary source due to its high graphite, refractory, and fluoride contents. Considering the rich material amount and criticality of CaF_2 which is the main feedstock for almost all fluorochemicals, SPL from primary aluminium production is one of the crucial wastes for recovery, reuse, and recycling in a circular economy.

1.3.1. SPL recycling

Previous studies have aimed to treat SPL to avoid disposal and create a valuable product. One of the first industries to use SPL is the cement industry, to improve firing conditions, but there are restrictions on the sodium content allowed. The mineral wool, iron (as an additive) and steel (as a substitute for fluorite) industry also use SPL. The problem with these uses is that only relatively small amounts of SPL may be used, to avoid complication in the process [10]. All these approaches necessitate separation of the main components carbon, brick, and fluorides.

Generally, two groups can be distinguished in terms of SPL recycling: Pyrometallurgical which involves high temperature processes or hydrometallurgy where aqueous solutions are used to extract metals, as is the case with leaching. Only some of these treatment technologies have been developed on an industrial scale. With the literature consulted, three SPL treatment

processes have been found which focus on converting fluorides into insoluble calcium fluoride and destroying cyanides [7].

1.3.1.1. High temperature (Pyrometallurgical) recycling

The use of SPL has been studied as an alternative to coal in blast furnaces as a result of the high content of graphite carbon present inside SPL. SPL has been found to have sufficient potential to release energy during combustion and can be considered as an alternative fuel. The high temperature of the combustion process ensures that cyanides are destroyed and fluorides are reduced in the exhaust gases, thus reducing the toxicity problems of SPL [11].

Fluoride can be recovered as an HF gaseous effluent. The downside of heat treatment is that it is a complicated treatment in operation and the valuable carbon source is not reused [12].

One of the largest SPL processing facilities in the world with the capacity to treat over 100,000 tons per year is located in Gum Springs in Arkansas, USA. SPL is mixed with limestone and sand and treated in the furnace for 90 minutes at temperatures between 500 and 800°C. Cyanides are thermally destroyed while soluble fluorides form calcium fluoride by reacting with the limestone. The resulting SPL waste remains hazardous due to its caustic nature. For this reason, possible opportunities for this treated SPL are being identified [7].

1.3.1.2. Hydrometallurgical recycling

Chemical leaching is proposed as a valid option for SPL treatment. Some researches have chosen the recovery and purification of carbon and cryolite separately by alkaline and acid leaching of SPL,which can reach a purity of 96% of each [12].

The most developed process involving chemical conversion to valuable products is the Low-Caustic Leaching and Liming (LCL&L) developed by Rio Tinto Alcan, Québec. This plant treats 80,000 tonnes of SPL annually. First, the SPL is ground and exposed to a low caustic fluoride and cyanide leach. Cyanides present in the leachate are destroyed by high pressure and temperature hydrolysis. Soluble sodium fluoride is concentrated and crystallized by evaporation and then reacted with lime to generate inert calcium fluoride and caustic. The caustic solution is recycled in the same process. The by-product obtained is to be valorized for the cement industry and the CaF_2 is taken to a drying system to reach a humidity of 10% to obtain a product with a higher value.

Thus, the LCL&L process produces three recoverable by-products: carbonaceous by-product, fluorides in the form of sodium or calcium fluoride and a caustic solution [7,13].

Another of the industrial processes developed is carried out by Befesa, which has a treatment capacity of 630,000 tons in five plants. Befesa uses a mixture of SPL and salt slags as raw materials in its processes. This material is ground and chemically treated to destroy cyanides, nitrides and carbides. The crushed SPL reduces the energy required to carry out the process. The solids are then filtered and a soluble NaCl/NaF component is added to the salt to treat the slag

to obtain an insoluble component suitable for the industry. In this process, no other residues are formed and the final product obtained is no longer dangerous [7].

1.4. Sources of NaF

The use of compounds containing fluorine has been increasing in the industry, and sodium fluoride (NaF) is the most widely used compound. Its consumption also causes an increase of fluorides in the wastewater. Excess fluoride in wastewater and drinking water can cause a health hazard and must be treated to reduce its concentration to a desirable value. WHO recommends 1.5 ppm of fluoride in drinking water as the maximum permissible contaminant level (MCL).

Therefore, other sources of NaF to obtain CaF_2 from its precipitation can be the treatment of wastewater. For example, NaF was obtained from the titanium processing washing wastewater [14].

Besides that, it is possible to obtain a high NaF stream doing water leaching of SPL, as a result of the high solubility of NaF in water. By doing this aqueous leaching, no obvious migration of other components of inorganic substances other than Na and F has been obtained [15].

1.5. Fluorides

Fluorspar or fluorite (CaF_2) is one of 27 critical raw materials for the EU because the risks of supply shortages and their impact on the economy are greater than for most other raw materials. In fact, there are about 10 years of fluorite stocks in the EU at the current rate of consumption; and less than 35 worldwide [16]. Its market price is on a long-term upward trend [10].

Overall, about 810 ktonnes of fluorite is consumed industrially in Europe. The main uses are in the metallurgical, ceramic and chemical industries. CaF_2 is used for the production of hydrofluoric acid (HF) and aluminium fluoride (AlF_3); as a flux in the manufacture of steel or the production of primary aluminium, the manufacture of enamels, glass, in coatings for welding rods, in the production of cement, in the production of insulators or refrigerants, among other uses and products [16].

Moreover, CaF_2 is especially added to sodium cryolite in the amount of 3-5 wt%, mainly to reduce the temperature of the liquid electrolyte. For this reason, the separation of calcium fluoride from SPL has an important value in the aluminium production process, as a product to be reused [17].

The following Figure 2 shows the distribution of CaF_2 consumption according to its importance.

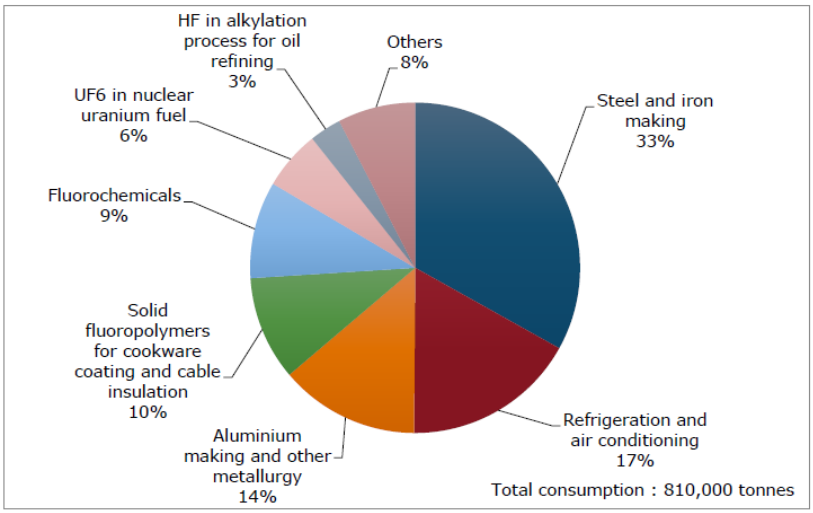

Figure 2 Uses of fluorspar in EU [16].

Industrial recycling of fluorine is globally very limited because fluorine-containing waste is mostly treated for the elimination of this compound and not for recycling.

The fluorine compounds contained in SPL come mainly from cryolite and sodium fluoride in the electrolyte used during the electrolysis process. Fluorides are present in both SPL cuts with typical ranges of 5-20wt%. They tend to concentrate in the lower carbon block at the point of contact with the molten fluoride salt [7].

Due to the presence of fluorides, when SPL comes into contact with acids it can release toxic gases such as hydrogen fluoride (HF). As for storage, concerns about fluoride are related to its potential for leaching and contamination of groundwater or the surrounding environment. Fluoride is toxic to aquatic and terrestrial organisms as it inhibits enzyme activity and is the main cause of dental and skeletal fluorosis in vertebrates [8]. For this reason, appropriate storage and handling protocols for fluorides should be followed.

In order to extract the fluorides from SPL, previous research has shown a 96% extraction of fluorides using solutions of $Al(NO_3)_3{\cdot}9H_2O$ and HNO_3. Generating a solid residue that largely contains Na_3AlF_6 and CaF_2, as the main fluorine species. This residue is subsequently treated with HNO_3 and $Al(NO_3)_3$ at 60°C to produce AlF^{2+} and AlF_2^+ with the aim of extracting the greatest amount of fluoride present in the SPL [8,15,18].

Fluoride has also been treated by precipitating aluminium hydroxyfluoride (AHF) with the addition of sodium hydroxide and controlling the pH. AHF is the precursor of aluminium fluoride, which is necessary for the production of aluminium. This process also involves carrying out the study to avoid coprecipitation of other minerals that are not of interest [19].

For the same purpose, chemical fluoride leaching has also been employed using diluted NaOH, H_2O_2, H_2SO_4 leachants at room temperature. The acid and caustic leachates obtained are combined and pumped through an ion exchange resin to selectively extract the aluminium and fluorine components. Then these two components were melted using NaOH to obtain a possible current for the study of synthetic cryolite [10].

In another study, the presence of CaF_2 has been shown to increase in the bottom ash after the co-incineration of SPL. These ashes contain NaF and Ca compounds, which when reacting produce CaF_2 [20].

From the point of view of this work, further studies on precipitation thermodynamics, the influence of pH and temperature are recommended to identify the conditions that lead to a high yield of fluoride extraction and CaF_2 generation.

2

THEORY

2.1. Fluoride recovery methods

Different methods can be used to remove the fluoride ion from an aqueous system, such as ion exchange, precipitation and coagulation principles, adsorption-based methodologies, reverse osmosis or crystallization.

If a dry sludge is to be obtained, crystallization could be a good choice since dewatering costs would be avoided, reducing the cost of operation. Although it is a complex process, since different factors such as fluid dynamic conditions, the nature of the seeds and oversaturation must be controlled [21]. Despite high values of fluoride recovery have been obtained by applying a thermal treatment to treat wastewater which contains fluoride using $Ca(OH)_2$ as a mineralizer, this treatment is not considered effective because it must be carried out at temperatures up to almost 200°C [22].

Adsorption is another approach to recover the fluoride from water. Different methodologies have been investigated where fluoride adsorbing material such as activated alumina or activated carbon should be used. The removal of fluoride by activated alumina depends on the pH and should be between 5 and 7 [23]. These investigations have shown that it is not cost-effective to treat wastewater with high fluoride concentration by adsorption due to the high consumption of the adsorbent and the high cost of regenerating ion exchange resins.

On the other hand, ion exchange has been found to be an efficient process when the solution has a high initial fluoride concentration [24].

In the case of reverse osmosis, it has minimal chemical consumption and removes other contaminants, but often pre-treatment is required and the membrane may become contaminated with other organic and inorganic compounds by removing more chemicals [25].

2.1. Precipitation process

Precipitation is a rapid formation of a sparingly soluble or amorphous solid-phase crystalline from a liquid solution phase. It involves the simultaneous of nucleation and subsequent growth from processes such as maturation and agglomeration. The physical and chemical properties of the crystallized solid depend on the size, shape, desired crystal and chemical purity [26].

In precipitation, the precipitates formed are usually not very soluble and are produced under conditions of high supersaturation.

First, supersaturation must occur in a solid free solution. This supersaturation often results from a chemical reaction.

Secondly, a progressive accumulation of supersaturation produces nucleation, that is, the formation of several small crystals (process b, Figure 3). A nucleus can be defined as the minimum amount of a new phase capable of independent existence and it is a complex of atoms that have passed an energy level that allows them to maintain their arrangement within the liquid. This group of atoms will not be able to stay together unless they reach a certain size. There are two types of nucleation: homogeneous when several atoms join together and form a nucleus completely enclosed in liquid; or heterogeneous when the nucleus forms on impurities, on the surface of the material that contains it or other materials that decrease its free energy required to form a stable nucleus. Normally the actual solidification processes begin due to heterogeneous nucleation [27].

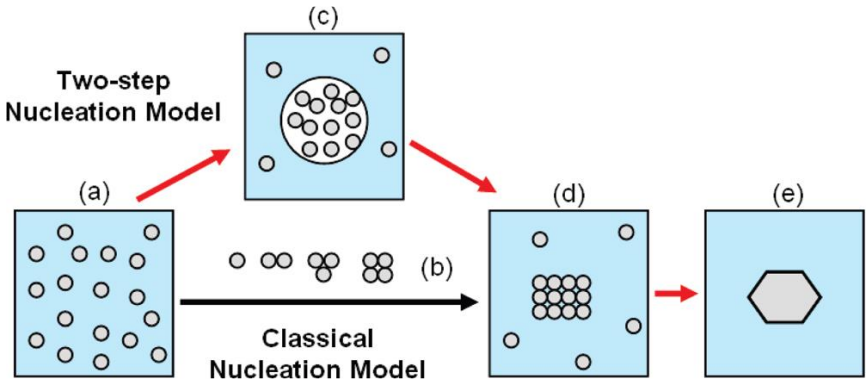

Figure 3 Proces from solution to solid crystal [26].

Thirdly, as a result of the high concentration of particles and the small size of the crystals, the resulting precipitate can be modified from maturation or aggregation [28]. This growth stage is governed by the diffusion of particles.

The classical theory of the nucleation process ignores the collision between two groups and assumes that clusters evolve in size by individual molecules. These defects suggest that nucleation follows a more complex process: The alternative two-step model, where the first step is the formation of a group of soluble molecules of sufficient size and the second step is the reorganization of that group into an orderly structure (process c, Figure 3) [26].

When the material has impurities due to the presence of atoms of different chemical nature, granules with different crystalline structure can be formed. The group of granules that have the same crystalline structure and the same properties is called a phase. The combination of the different phases defines the properties of the material.

The different phases of a material can be seen in a phase diagram. These are graphs that can show the start and end point of the process after an infinitely long time, but cannot show how fast the process is.

2.2. Precipitation of CaF_2

Most treatment processes have high energy demands and they do not use their full potential as a source of fluoride. Precipitation is considered a simple and cost-efficient method of removing fluoride from aqueous streams as it can be done at room temperature and without modifying the initial pH of the solution. This is because it has been determined that the pH does not affect the efficiency of fluoride removal in the range of pH > 4 and the aqueous stream to be treated is highly basic [29]. Therefore, the use of precipitating agents to obtain CaF_2 is not considered as an expensive process [15].

On the other hand, CaF_2 and $Al(OH)_3$ precipitates result in small particles that take a certain time to sediment, which will require large sedimentation clarification tanks if it is reproduced at the industrial scale. Also an overdosing of coagulation agents results in high chemical costs and an excess of wet sludge. In addition, the removal of fluoride by precipitation generates large quantities of water-rich sludge [21].

One of the most important negative aspects of CaF_2 precipitation is the competitive precipitation of other minerals that are not of interest [19]. If these impurities are to be removed, an additional purification step needs to be added to the process.

As is the case with the study of CaF_2 precipitation from concentrated hexafluorosilic acid wastewater by adding calcium hydroxide. When a higher fluoride yield was obtained, the sludge contained impurities such as SiO_2 and $CaSiF_6$. This fact required a purification to reach a higher degree of CaF_2. Silicon dioxide was removed from the CaF_2 surface by alkaline precipitation with NaOH [30].

2.3. Thermodynamic modelling

Solution speciation models have been designed to study a wide range of aqueous solutions in chemical, geochemical and environmental systems. These models have significant industrial importance to predict the effect of factors such as temperature, pH or ion concentration.

In an equilibrium system, solution speciation is affected by the overall concentration of the ion species and the interactions between them. Therefore, the equilibrium of a reaction is defined by the thermodynamic equilibrium constant, that only depends on temperature and pressure. These are defined by the terms of concentration.

The thermodynamic analysis using the HSC software is based on enthalpy (H), entropy (S), heat capacity (Cp) or Gibbs energy (G) values for chemical species.

The mutual stability of species must be done using Gibbs energy, as defined by Equation (1).

$$\Delta G^\circ = \Delta H^\circ - T \cdot \Delta S^\circ \qquad (1)$$

Gibbs Free Energy is the useful work that a system that evolves from an initial state to a final one is capable of doing. The Gibbs Free Energy in standard conditions allows us to predict if the reaction will occur only in standard conditions [31].

However, the standard conditions of a chemical reaction only last for a moment. As the reaction progresses, the concentration of the reagents varies and the system no longer has a free energy ΔG° but ΔG. The relationship between the free energy of reaction at any moment in time (ΔG) and the standard-state free energy of reaction (ΔG°) is described by the following equation.

$$\Delta G = \Delta G° + RT \cdot \ln Q \qquad (2)$$

Where, R is the ideal gas constant in units of J/mol·K, T is the reaction temperature in Kelvin and Q is the reaction quotient at that moment in time.

When a chemical reaction is in equilibrium and it reverses its direction, the free energy is 0 (ΔG = 0). Under these conditions, the reaction quocient becomes the equilibrium constant and the reaction equilibrium constant is calculated with the following equation.

$$\Delta G° = -RT \cdot \ln K \qquad (3)$$

This equation allows to calculate the equilibrium constant for any reaction from the standard-state free energy of reaction, or vice versa.

By relating ΔG° to K, it is found that the magnitude of ΔG° tells how far the standard state of equilibrium is. The smaller the value of ΔG°, the closer the standard state is to equilibrium. The higher the value of ΔG°, the further the reaction has to go to reach equilibrium. So, if ΔG<0 the reaction occurs spontaneously.

Focusing on the equilibrium constant, if the value of K is greater than 1, it will imply that the reaction has reached equilibrium and a considerable amount of product has been formed. This will result in Ln K being a positive value [31].

2.4. Stability diagram

It is important to predict the stability of the chemical compounds to perform the thermodynamic study. The chemical reactions in an aqueous medium are not usually dominated by a single process, but generally involve several different semi-reactions depending on the pH, for example. There are several factors that affect the stability of chemical compounds: initial concentration of each element or compound, the concentration of the added product, pH and temperature. To study the effect of these factors, HSC Chemistry 9 was used to plot Pourbaix diagrams, Equilibrium diagrams and diagrams for the ΔG-free energy of reactions [32].

2.4.1. Pourbaix diagram

A potential-pH (or E-pH) diagram, also known as a Pourbaix diagram, is a graphical representation of thermodynamic conditions as a function of electrode potential (ordinate) and pH (abscissa).

Although initially the diagrams were calculated for pure metals in pure water at 25°C, the advances allowed to include ionic species and temperatures. The diagram takes into account

chemical and electrochemical equilibria as well as solubility products; and they are constructed from calculations based on the Nernst equation and the equilibrium constants.

Following the Nernst equation, the standard potential (E^0) is given by the equation (4):

$$\Delta G° = -n\ F\ E° \qquad (4)$$

Where n is the number of exchanged electrons, F is Faraday constant (96,485 C/mol) and ΔG^0 is the standard Gibbs free energy for reactions (J).

If considering the Nernst equation and Gibbs free energy, equation (3) and (4) in equilibrium conditions, it is found:

$$E° = -\frac{R\ T}{n\ F} \ln K \qquad (5)$$

It shows the stability areas of several types of species of a certain element, such as dissolved ions, condensed oxides, hydroxides, oxides, etc [32]. The defined areas are not the only areas where a certain species exists, but where it is predominant. The separation lines between species are established where the activity of these two species is equalized because it corresponds to the area where they exist in equilibrium. The presence of each species extends to neighbouring areas, decreasing very significantly.

In the Pourbaix diagrams, the stability zone of water in relation to oxygen and hydrogen is determined, as can be seen in Figure 4. The upper limit is represented by the oxygen reduction reaction to water (b). Above this limit, water is thermodynamically unstable with respect to the generation of oxygen gas. The lower limit is defined by the hydrogen reduction reaction (a). Below this line, water is thermodynamically unstable with respect to the generation of hydrogen gas.

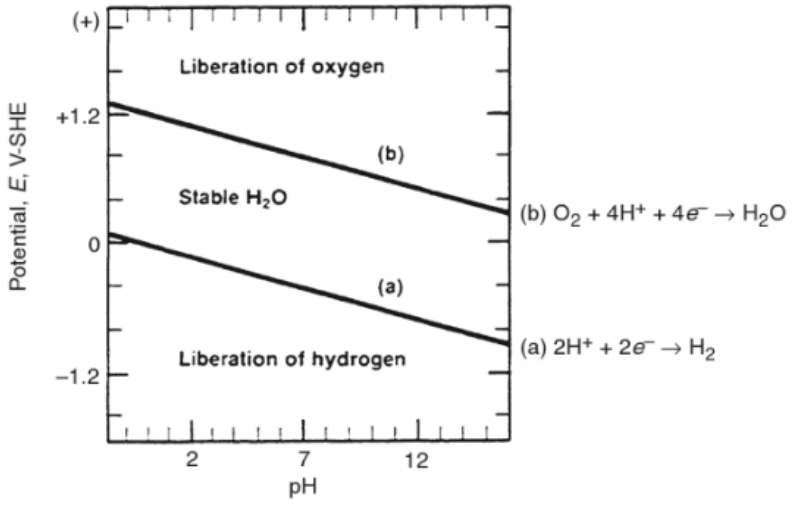

Figure 4 Potencial-pH diagram for water [33].

The potential-pH diagram can be divided into four regions. Vertically it can be divided at pH 7, separating the alkaline zone from the acidic zone. Horizontally, the upper region is oxidizing and the lower region is reducing [33].

The analysis of these diagrams allows us to predict which types of species can coexist in different environments. It is important to know which species is predominant in order to know which reaction is produced in the system and if the desired product, CaF_2, is obtained as the final product.

2.4.2. Equilibrium diagram

The HSC Equilibrium module is used to calculate the equilibrium compositions of multiple components in the study systems. The amounts and temperatures of the raw materials are specified, to make a study according to the amount of precipitation agent or water added or depending on the temperature of the system.

2.5. Sample Characterization

Two techniques have been used to study and identify the solid obtained experimentally: Fourier transform infrared spectroscopy (FTIR) and X-ray powder diffraction (XRD).

2.5.1. Fourier Transform Infrared Spectroscopy analysis FTIR

Fourier transform infrared (FTIR) spectroscopy is an instrumental method based on measurement of the vibration of a molecule excited by infrared radiation at a specific wavenumber range. When IR radiation is passed through a sample, some radiation is absorbed by the sample and some passes through (is transmitted). This transmitted radiation is detected in the spectrum [34].

This spectrum shows the wavelengths which the sample absorbs energy, corresponding to the vibration of the bonds. In this way, the bonds present in the sample can be determined to identify the chemical structure of the molecule. The concentration of the sample components can also be calculated [34].

This technique is an easy way to obtain transmission spectra of organic, polymeric and, in some cases, inorganic materials.

2.5.2. X-Ray powder Diffraction XRD

X-ray diffraction is a non-destructive technique for characterizing crystalline materials. It provides structural information such as chemical composition, crystal structure, crystal size, deformation, preferred crystal orientations and layer thickness [35].

XRD peaks are produced by constructive interference of a monochromatic beam of X-rays scattered at specific angles from each set of lattice planes in a sample. The peak intensities are determined by the atomic positions within the lattice planes [35].

Using a standard database of diffraction patterns, the phases of a crystalline sample can be identified.

3

METHODS

In this work a study of thermodynamic modelling has been carried out first, using software and then verifying these results experimentally. This chapter presents the methods used in the work of this thesis.

3.1. Thermodynamic studies

HSC Chemistry 9 software developed by Outotec was used for the thermodynamic study of the process for each of the precipitating agents.

The program was used to draw the Pourbaix diagrams, energy reaction diagrams ΔG and to perform the study of the equilibrium compositions and the temperature of the products obtained.

Initially, it was planned to carry out the same study to check the results using the PHREEQC software. But it was found to have a limitation, that compounds such as $CaCl_2$, $Ca(OH)_2$ or $NaAl(OH)_4$ are not in the database.

3.2. Sample preparation

In order to study the precipitation of the different precipitating agents, an artificial sample has been prepared with the same characteristics as the input solution. This solution should be composed of NaOH, NaF and $NaAl(OH)_4$.

To prepare the $NaAl(OH)_4$ solution, NaOH and $Al(OH)_3$ are used following the reaction [36]:

$$NaOH + Al(OH)_3 \rightarrow NaAl(OH)_4$$

Aluminium hydroxide is practically insoluble in water but it can be dissolved in aqueous NaOH solutions at temperatures near the boiling point [37,38].

The artificial input solutions were prepared by first dissolving NaOH and NaF to create a basic environment necessary for the subsequent dissolving of $Al(OH)_3$. NaOH and NaF were mixed at room temperature with MilliQ deionised water to the desired volume of the initial solution. The mixture was agitated using a hotplate/stirrer until the added reagents were dissolved at room temperature. The desired amount of $Al(OH)_3$ was then added to the mixture and heated to boiling point and held at this temperature for 10 min with agitation using a stirrer. This process has been carried out following the consulted bibliography [36].

Due to the low solubility of $Al(OH)_3$ in the prepared basic environment, when the solution was cooled down there were traces of $Al(OH)_3$ that precipitated. For this reason, it was decided to filter the solution through Fisherbrand QL100 filter paper. The amounts of precipitated $Al(OH)_3$ are not shown because the amount of precipitated $Al(OH)_3$ is not statistically correct due to the low amounts. In the end, MilliQ deionised water was added to form the solution with the required volume. The solution was stored until use.

The reagents used to prepare the artificial sample and the precipitation reactions (NaOH, NaF, $Al(OH)_3$, $CaCl_2$, $Ca(OH)_2$, $CaCO_3$) have been purchased from Sigma-Aldrich, Ltd. $Ca(OH)_2$ has 96% purity and contains max. 3% $CaCO_3$. $CaCl_2$ has 96% purity and contains max. 4% magnesium and alkali salts. $CaCO_3$ has 99% purity and contains max. 0,0005% phosphorus. NaOH has 97% purity and contains max. 1% Na_2CO_3. NaF has 99.9% purity and $Al(OH)_3$ is pure.

All aqueous solutions were prepared using MQ water with resistivity equal to 18.2 mΩ·cm at 25°C and total organic content <5 mg/L.

3.3. Precipitation reactions

The precipitation reactions were carried out at room temperature and with constant agitation by using a magnetic stirring plate at 500 rpm.

The pH of the initial solution (without precipitating agent) was measured and after the addition of the precipitation agent every 15 min, to observe a variation of this. As the solution was expected to be highly alkaline, the pH values were measured semiquantitavely by visual comparison of the Dosatest pH test strips.

After 3 hours of adding the precipitating agent, the agitation was stopped and the mixture was left to stand. When the agitation was stopped, precipitation started to be observed in the samples.

When 20 hours had passed since the addition of the precipitating agent, the separation of the obtained precipitate began. First the top of the liquid was taken by a pipette without mixing the powder. The bottom part was then transferred to a test tube and centrifuged using a OHAUS Frontier FC5714 Multi-Pro centrifuge for 10 minutes at 3000 rpm.

Subsequently, to finish separating the liquid part, the liquid phase was removed from the test tube by pipette. Finally, the test tube was introduced into the laboratory oven at 40°C to dry the solid. Once the precipitate was dry, it was weighed and the characterization techniques were performed.

3.4. Sample Characterization

3.4.1. X-Ray powder Diffraction XRD

An X-ray diffractometer (XRD, D8 ADVANCE, Bruker) with Cu Kα radiation (40KV and 40mA) was used. X-ray diffraction is a non-destructive technique that provides information such as

structures or phases to characterize crystalline materials. Using a standard database, the phases of the crystalline sample can be identified.

When the sample to be analysed was small, a thin layer was applied to the sample carrier by dropping a suspension of the material in acetone and allowing it to evaporate.

3.4.2. Fourier Transform Infrared Spectroscopy analysis FTIR

A Perkin Elmer Spectrum Two FTIR Spectrometer was used to detect the composition of the precipitate. Chemicals used in the experiments were also analysed to check their spectrum and purity.

The spectrometer is equipped with a deuterated triglycine sulfate (DTGS) detector and with a monolithic diamond ATR accessory (PerkinElmer, UATR two).

4

RESULTS

4.1. Input flow

This study is focused on the treatment of fluoride from the process water of an SPL recycling process. The input flow for the fluoride precipitation unit is defined by the pre-treatment of the process. The input stream has the following composition:

Table 1 Input flow data.

Input flow			*Mw g/mol*	*kg/L*	*mol/L*
Mass flow	51.161	kg/h			
Volume	49.235	L/h			
H_2O	49.944	kg/h	18.015	1	55.50844
$NaOH_{(a)}$	0.106	kg/h	39.997	0.00212	0.05306
$NaF_{(a)}$	0.005	kg/h	41.988	0.00010	0.00238
Na^+	0.559	kg/h	22.990	0.01119	0.48685
F^-	0.091	kg/h	18.998	0.00182	0.09590
$NaAl(OH)_{4(a)}$	0.123	kg/h	118.001	0.00246	0.02087

The behavior of the solution has been studied from water leaching investigations to know the composition of the ions. The alkaline compound NaOH dissolves as a strong electrolyte where it is completely dissociated, following the reaction (6). In the case of salts, they are dissociated into ions, equation (7) and equation (8)[39].

$$NaOH_{(a)} \rightarrow Na^+ + OH^- \quad (6)$$

$$NaAl(OH)_{4\,(a)} \rightarrow Na^+ + Al(OH)_4^- \quad (7)$$

$$NaF_{(a)} \rightarrow Na^+ + F^- \quad (8)$$

The input flow has been calculated taking into account that the fluoride ion comes from a weak acid that can react with water giving a basic dissolution in chemical equilibrium.

$$F^- + H_2O \rightleftarrows HF + OH^- \quad (9)$$

The calculated pH value of the input stream at 25°C, taking into account $NaOH_{(a)}$, $NaF_{(a)}$ and $NaAl(OH)_{4(a)}$ concentrations only, is 12.62. This value has been calculated by numerical

calculations and applying a pH calculation simulator [40]. The calculated pH value is consistent with the value tested in the literature for a similar solution with pH values between 12.56 and 13.15 [15].

As can be seen, $NaAl(OH)_4$ is also present in the inlet flow. This complex component can present singular characteristics. The following section will focus on the behaviour of this component.

Aluminium can exist in several different forms depending on the pH, temperature, and the type of element with which it is in contact in water. Figure 5 shows the solubility of aluminium in contact with water for different pH values, which has been contrasted with that calculated by HSC (Figure 6).

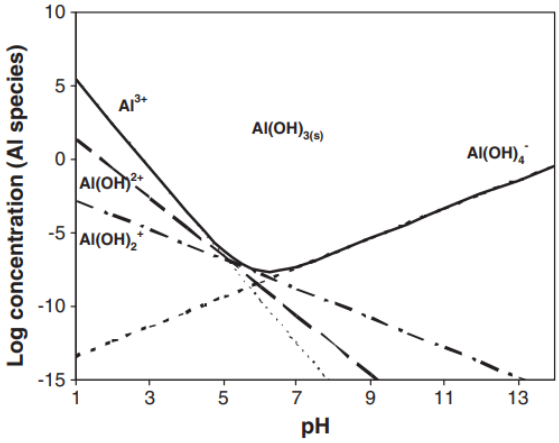

Figure 5 Solubility of aluminium hydroxide at various pH values [41].

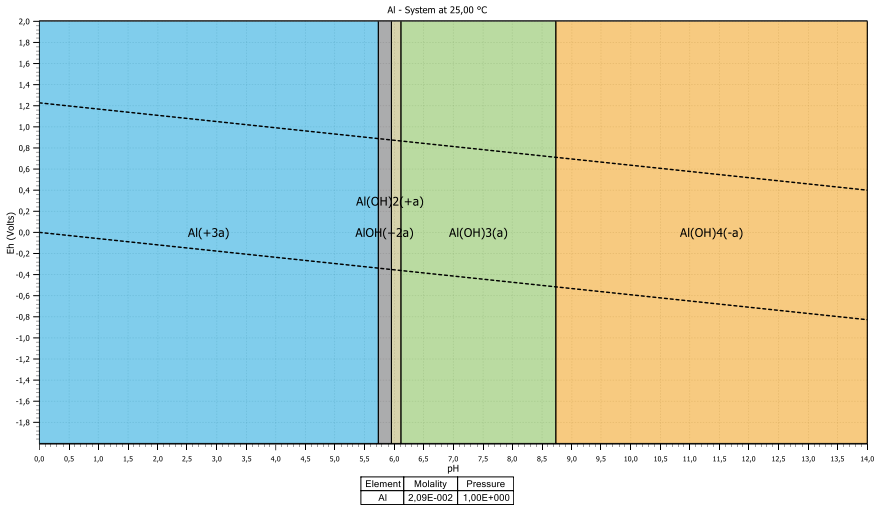

Figure 6 Behaviour of aluminium in contact with water for different pH.

At aluminium concentrations below 1.5 M and temperatures below 100°C, $Al(OH)_4^-$ is the only significant aluminium ion in alkaline solution, which forms by: [42,43].

$$Al(OH)_3 + H_2O \rightleftarrows Al(OH)_4^- + H^+ \qquad (10)$$

It is observed how the aqueous aluminium ion in anionic form, $Al(OH)_4^-$ can react with the Na^+ cation present to form Al complexes, $NaAl(OH)_4$. This is the predominant species as shown in Figure 7 for basic pH. The literature also shows how complex species are dominant [41,44]. This solution only exists in the presence of appreciable concentrations of $NaOH_{(a)}$, because the binary $NaAl(OH)_{4(a)}$ solution is unstable with respect to aluminium precipitation [45].

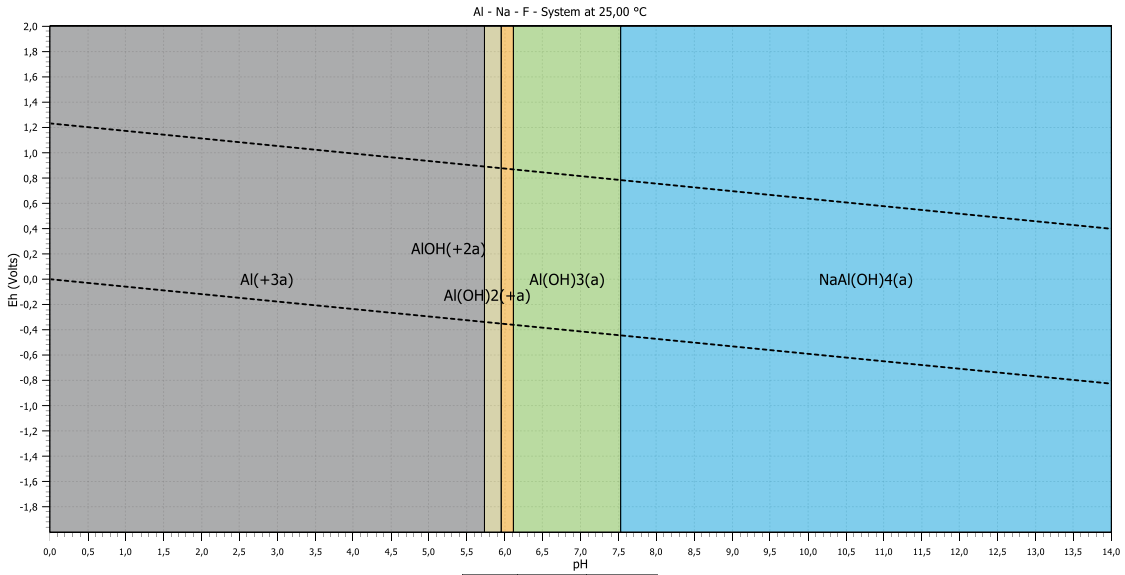

Element	Molality	Pressure
Al	2,09E-002	1,00E+000
Na	2,09E-002	1,00E+000
F	2,09E-002	1,00E+000

Figure 7 Solubility of $NaAl(OH)_4$ for different pH.

If the input flow is studied in its totality, it is observed that $NaAl(OH)_{4(a)}$ is the predominant species for the elements of Na and Al, while F^- is the predominant species for the fluoride (Figure 8). Thus it is significant to include $NaAl(OH)_{4(a)}$ into the thermodynamic calculations of the precipitation process due to possible side reactions that can affect the final product.

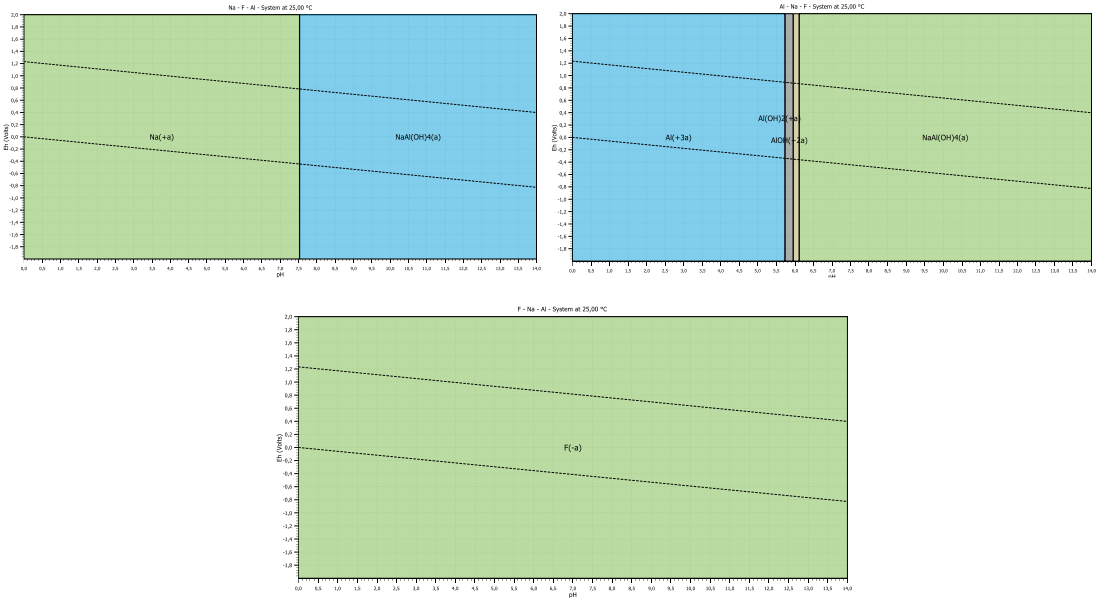

Figure 8 Input flow solubility, according to the elements Na, Al and F.

4.1.1. Reaction between components

The following reactions are proposed as possible reactions between species present in the input flow.

$$NaF + NaAl(OH)_4 \rightarrow NaOH + NaAlF_4 \quad (11)$$

$$NaF + NaAl(OH)_4 \rightarrow NaOH + AlF_3 \quad (12)$$

$$NaF + NaAl(OH)_4 \rightarrow NaOH + AlF_3 + Al(OH)_3 \quad (13)$$

In order to know if these reactions occur, the HSC Chemistry Reaction model has been used. Changes of standard Gibbs free energies by time for the mentioned reactions are given in Figure 9. It is assumed that the reaction (11) given in green line, is not spontaneous considering the high ΔG values, which indicate that the reaction is far from equilibrium, as well as the logarithm of the reaction constants which are lower than 0, fact that in the equilibrium the reagents are more favourable than the products.

(a)

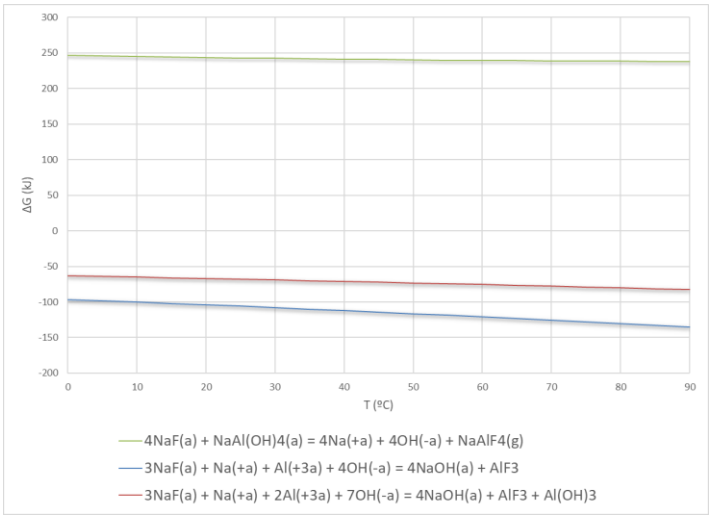

(b)

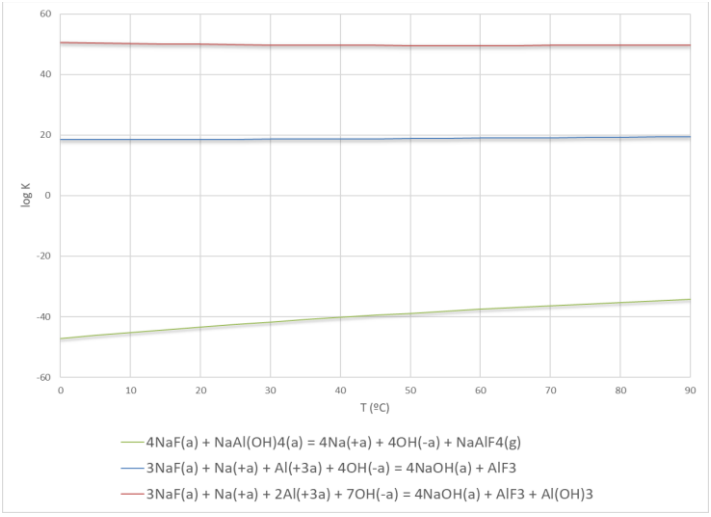

Figure 9 (a) Gibbs free energy and (b) reaction equilibrium constant changes by the temperature of possible reactions between components.

In relation to reaction (12) and (13) in blue and red colour respectively, they have only been spontaneous when the reacting species is Na^+, Al^{3+} and OH^- like $NaAl(OH)_4$. As demonstrated above, $NaAl(OH)_4$ does not dissociate giving these ions. For this reason, no reaction is found to be possible between the components of the input flow.

4.2. Precipitation with $CaCO_3$

First, the solubility of $CaCO_3$ in the input current was studied using the PHREEQC software. The results calculated by PHREEQC is shown in Table 2.

Table 2 Input and output data for $CaCO_3$ in PHREEQC.

```
EQUILIBRIUM_PHASES 1
    Calcite    0 10
SOLUTION 1
    temp       25
    pH         7
    pe         4
    redox      pe
    units      mmol/kgw
    density    1
    -water     1 # kg
```

```
-------------------------------Phase assemblage-------------------------------

                                                        Moles in assemblage
Phase               SI  log IAP  log K(T, P)   Initial       Final       Delta

Calcite           0.00    -8.48     -8.48    1.000e+01   1.000e+01  -1.230e-04

-----------------------------Solution composition-----------------------------

      Elements           Molality       Moles

      C                1.230e-04   1.230e-04
      Ca               1.230e-04   1.230e-04
```

In the output data, it can be seen that the solubility (Delta) of calcite, $CaCO_3$, is $-1.23 \cdot 10^{-4}$ mol/L. The negative symbol indicates that it has dissolved in the given amount which indicates the limited dissolution of the $CaCO_3$.

The dissolved moles of calcium and carbonate correspond to the equilibrium present in the reaction of the calcite solution, being the same value of solubility as the moles of each ion.

$$CaCO_3 \rightleftarrows Ca^{2+} + CO_3^{2-} \qquad (14)$$

4.2.1. Proposed reactions

When the input current has contact with $CaCO_3$, the following reactions are proposed. Mainly, it is expected that $CaCO_3$ will react with NaF to obtain Na_2CO_3 and CaF_2 as the equation (15).

Reactions (15), (17),(18),(19) and (20) are considered main reactions and reaction (16) is considered side reaction.

$$NaF + CaCO_3 \rightarrow Na_2CO_3 + CaF_2 \qquad (15)$$

$$NaOH + CaCO_3 \rightarrow Na_2CO_3 + Ca(OH)_2 \qquad (16)$$

$$NaAl(OH)_4 + CaCO_3 \rightarrow NaAlCO_3(OH)_2 + Ca(OH)_2 \qquad (17)$$

$$NaAl(OH)_4 + CaCO_3 \rightarrow Al(OH)_3 + Ca(OH)_2 + Na_2CO_3 \qquad (18)$$

$$NaAl(OH)_4 + CaCO_3 \rightarrow Al_2(CO_3)_3 + NaOH + Ca(OH)_2 \quad (19)$$

$$NaAl(OH)_4 + CaCO_3 \rightarrow Al_2(CO_3)_3 + Na_2CO_3 + Ca(OH)_2 \quad (20)$$

All the possible species for each compound have been taken into account for the calculation of these reactions, which are separately given in Appendix aA. The same form of all the species has been maintained in each reaction studied. That is, the same reaction has been studied with all its compounds in the aqueous phase and also all of them in the ionic phase, never mixing these forms.

Gibbs free energy and equilibrium constants for the reactions were calculated using the HSC Chemistry software, for the temperature range between 0 and 90°C. The results are shown in Figure 10. Only the reaction with the species that have presented lower Gibbs energy value is shown, for each one of the reactions, because this is the most probable thermodynamically.

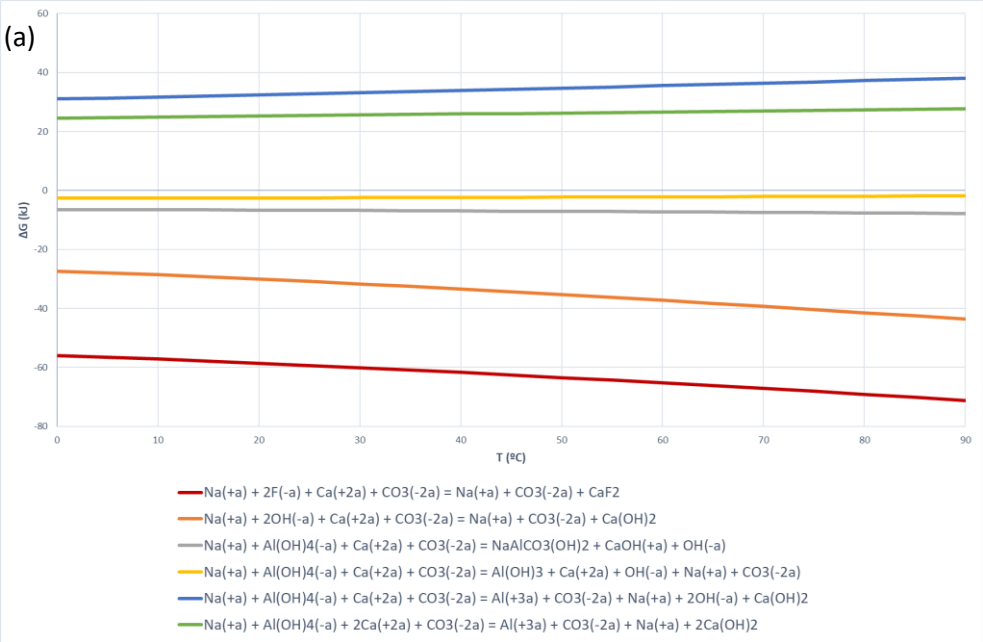

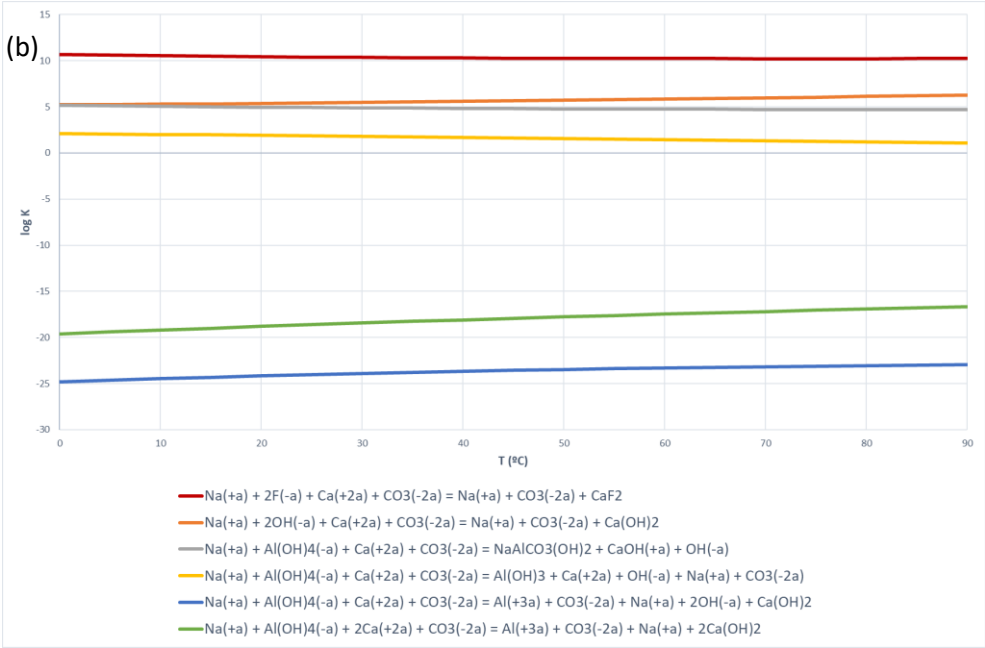

Figure 10 (a) Gibbs free energy and (b) reaction equilibrium constant changes by the temperature of possible reactions with $CaCO_3$.

The results show that the reaction (19) and (20), in blue and green respectively in Figure 10 (a), do not occur spontaneously because they present positive Gibbs free energy values for all the studied temperature range and negative values for the equilibrium constant logarithms.

The reaction (15), in red colour, is thermodynamically more stable because the Gibbs free energy for the equation has lower and negatives values at the study temperatures. It also corresponds to the reaction of interest which produces CaF_2 as a precipitate.

In Figure 10b, it can be seen that the reaction of interest has the highest logK values. When the values of log K are greater than 0, it indicates that the product will be formed since the product concentration is greater than the reagent concentration.

4.2.2. Equilibrium composition

GEM (Equilibrium Compositions Module) has been used to know the composition in equilibrium and to study until when the precipitation reaction is saturated. The input moles of the different components have been calculated with the data of Table 1 for 10,000h to simulate a large capacity process. Although high amounts were used for the calculation, the final percentage values obtained do not change for a small laboratory-scale system as a similar multiplication was applied to all species.

Table 3b shows this data calculated for both of these different time values.

Table 3 Input current characteristics.

(a)

Input flow			*Mw g/mol*	*kg/L*	*mol/L*
Mass flow	51.161	kg/h			
Volume	49.235	L/h			
H2O	49.944	kg/h	18.015	1	55.50844
$NaOH_{(a)}$	0.106	kg/h	39.997	0.00212	0.05306
$NaF_{(a)}$	0.005	kg/h	41.988	0.00010	0.00238
Na+	0.559	kg/h	22.990	0.01119	0.48685
F-	0.091	kg/h	18.998	0.00182	0.09590
$NaAl(OH)_{4(a)}$	0.123	kg/h	118.001	0.00246	0.02087

(b)

	kmol calculated for 10.000h	*Mw g/mol*	*kg*	*mol calculated for 1 h*
H_2O	27700	18.01	499023.26	2770
$NaOH_{(a)}$	27	39.99	1079.92	0.27
$NaF_{(a)}$	1.2	41.98	50.38	0.12
Na^+	243	22.99	5586.51	24.3
F^-	48	18.99	911.92	4.8
$NaAl(OH)_{4(a)}$	10.43	118.00	1230.75	1.043

Initially, the study has been carried out by adding $CaCO_3$ in 100 steps of 1kmol; and it is observed that the production of CaF_2 is saturated before stage 30.

Figure 11 shows clearly a first initial stage until 27 kmol of $CaCO_3$ is added. In this zone CaF_2, OH(-a), Na_2CO_3 and $NaAlCO_3(OH)_2$ are produced. It is also observed how the compounds F(-a), NaF, Na(+a) and $Al(OH)_3$ are consumed. This range ends when the highest equilibrium amount of CaF_2 is reached and from this point on, this amount becomes constant. This happens because there is no more NaF or F(-a) to be reacted. It can be considered that in this first stage the main reaction (15) takes place, among others.

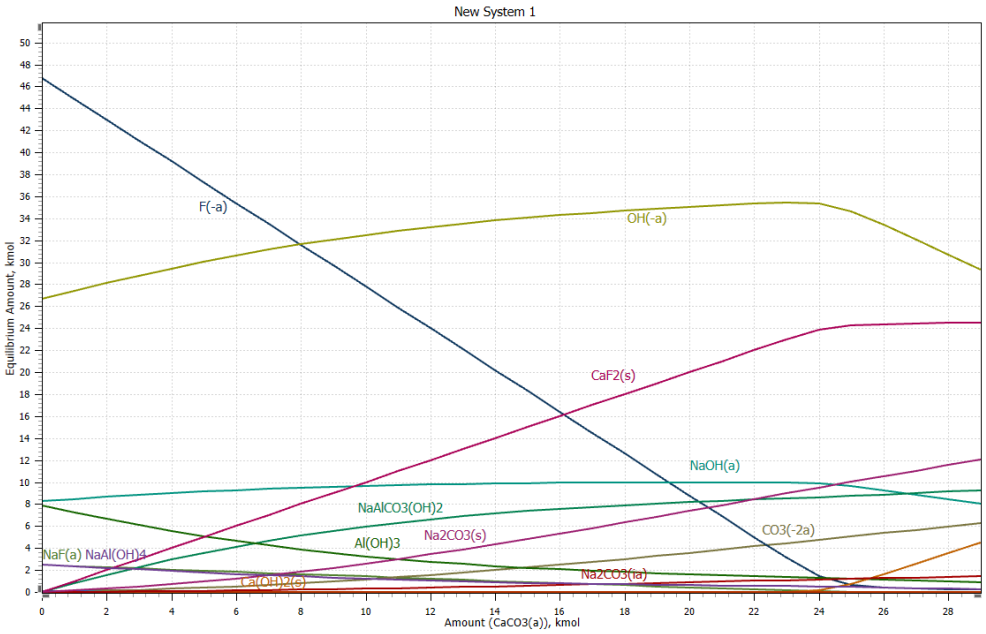

Figure 11 Evolution of the equilibrium amount of each component according to the added amount of $CaCO_3$.

In these graphs, the components of water and Na(+a) have been excluded as they made it difficult to observe the data by showing very high values compared to the other components. In the case of water, it is not modified by the introduction of $CaCO_3$. On the other hand, the amount of Na(+a) in equilibrium is reduced.

In Figure 12, solid compounds of CaF_2, Na_2CO_3, $Ca(OH)_2$, $Al(OH)_3$ and $NaAl(OH)_4$ are observed. Although a greater equilibrium amount of CaF_2 has been obtained. These compounds should be taken into account to study the composition of the solid obtained.

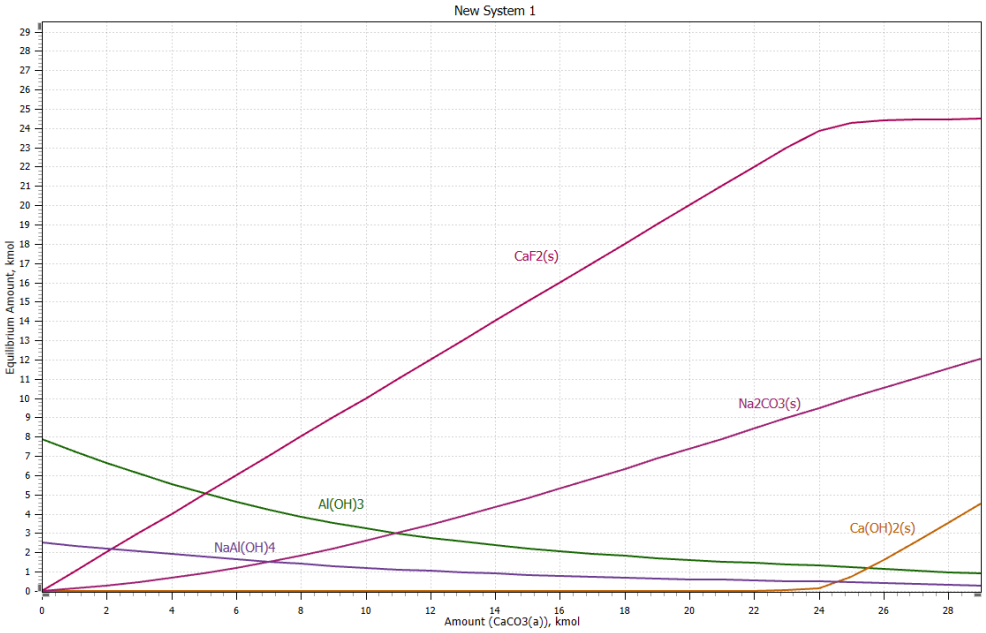

Figure 12 Evolution of solids compounds according to the added amount of $CaCO_3$.

Using the Equilibrium Compositions Module (GEM), a study has also been carried out modifying the temperature and the amount of water added.

When the temperature is modified between 20 and 50°C, as shown in Figure 13, no differences are observed in the equilibrium composition of different solids.

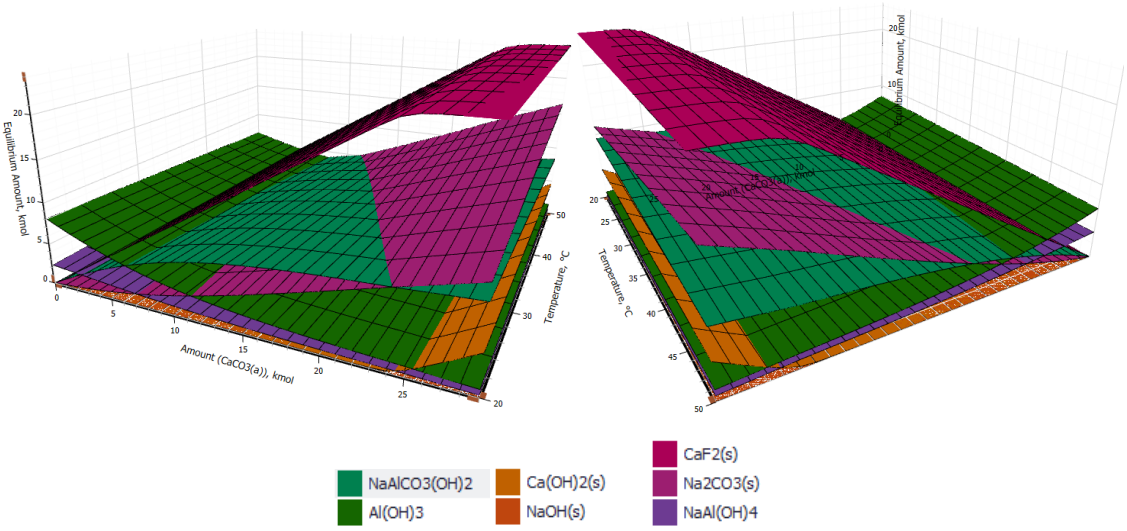

Figure 13 Evolution of solid components according to the added amount of $CaCO_3$ and temperature.

There are also no differences in the equilibrium compositions when water is added, as shown in Figure 14. In Appendix B, the graphs for the evolution of all the components studied are shown. In none of the cases, are differences observed when modifying these two variables.

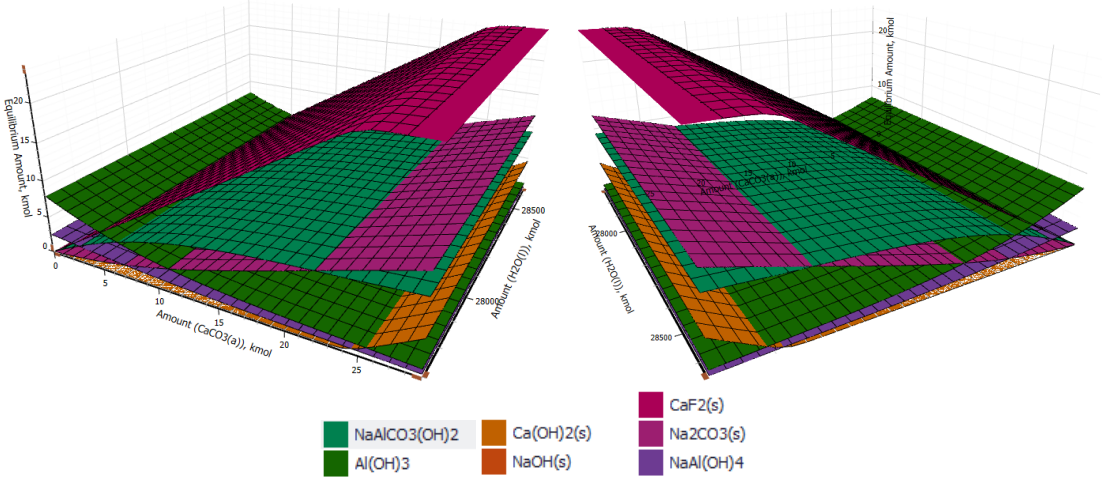

Figure 14 Evolution of solid compounds according to the added amount of $CaCO_3$ and water.

The optimal endpoint of the precipitation reaction is taken as step 28 with the addition of 27 kmol $CaCO_3$. To select this optimal point, the criterion that has been followed is that the production of CaF_2 is stopped when the increase between two consecutive steps is less than 0.5 kmol. Table 4 shows the composition of the final sample.

Table 4 Composition of step 28 with the addition of 27kmol $CaCO_3$.

	Equilibrium Amount	*Equilibrium Composition*
Species	kmol	mol fraction
NaF(a)	1.49E-02	5.32E-07
CaCO3(a)	8.24E-04	2.94E-08
Na(+a)	2.39E+02	8.51E-03
CO3(-2a)	5.65E+00	2.01E-04
Ca(+2a)	4.49E-05	1.60E-09
F(-a)	3.18E-01	1.13E-05
H2O(l)	2.77E+04	9.88E-01
NaAl(OH)4(a)	6.40E-03	2.28E-07
NaOH(a)	8.85E+00	3.16E-04
NaAlCO3(OH)2	9.01E+00	3.21E-04
Al(OH)3	1.06E+00	3.77E-05
Al2(CO3)3(a)	6.70E-69	2.39E-73
OH(-a)	3.21E+01	1.14E-03
Al(+3a)	4.03E-30	1.44E-34
Al(OH)3(a)	1.55E-09	5.54E-14
Ca(OH)2(ia)	2.53E-07	9.02E-12
Ca(OH)2(s)	2.57E+00	9.15E-05
NaOH(s)	9.97E-05	3.56E-09
CaF2(ia)	2.41E-12	8.59E-17
Na2CO3(ia)	1.32E+00	4.71E-05
CaF2(s)	**2.44E+01**	8.72E-04
Na2CO3(s)	1.10E+01	3.93E-04
NaAl(OH)4	3.59E-01	1.28E-05

The pH of the aqua phase has been calculated from the composition of the following species: $NaF_{(a)}$, $CaCO_{3(a)}$, $NaAl(OH)_{4(a)}$, $NaOH_{(a)}$, $Al(OH)_{3(a)}$, $Ca(OH)_{2(ia)}$, $Na_2CO_{3(ia)}$; obtaining a value of 12.20. In Appendix C, the data used for the calculation of this pH is shown.

For the solids, the CaF_2 purity has been calculated, obtaining a value of 40.7% and possible impurities are given in Table 5.

Table 5 Composition of solid obtained.

	Purity (%)
NaAlCO3(OH)2	27.67
Al(OH)3	1.76
Ca(OH)2(s)	4.05
NaOH(s)	0.00
CaF2(s)	**40.69**
Na2CO3(s)	24.92
NaAl(OH)4	0.90

With Heat and Material Balances Module (Bal) of HSC Chemistry, the temperature of the products obtained has been calculated, obtaining a temperature of 25.4°C.
As this temperature is close to the temperature value studied, the above results are considered acceptable.

Table 6 Result obtained from the Bal module.

Temperature of products = 25.4 °C (when Heat Balance = 0)

BALANCE	Amount kmol	Amount kg	Amount Nm³	Heat Content kWh	Total H kWh	EXERGY kWh
IN1	28056.6	5.11E+05	500.5	0.0	-2.24E+06	6338.1
OUT1	28035.4	5.11E+05	502.2	0.0	-2.24E+06	6191.3
BALANCE	-21.2	0.0	1.7	0.0	-181.0	-146.8

4.2.3. Washing stage

After precipitation, a subsequent washing stage is proposed to obtain a higher degree of CaF_2 purity. According to mass balance calculations, adding 381 L of water should dissolve all $NaAl(OH)_4$ and Na_2CO_3, as shown in Table 6. After this washing stage, the purity of CaF_2 can theoretically increase from 40.69 to 54.89%.

Table 7 Characterization of the washing stage.

	Initial amount (kg)	*Purity (%)*	*Solubility (g/L)*[46]	*Solubilized (kg)*	*Insoluble(kg)*	*Purity (%)*
				Adding 381L of water		
$NaAlCO_3(OH)_2$	1297.06	27.67	Insoluble	0	1297.06	37.32
$Al(OH)_3$	82.41	1.76	Insoluble	0	82.41	2.37
$Ca(OH)_2(s)$	190.08	4.05	1.59	0.605	189.48	5.45
$NaOH(s)$	0.004	0.00		0	0	0
$CaF_2(s)$	1907.65	**40.69**	0.17	0.065	1907.59	**54.89**
$Na_2CO_3(s)$	1168.37	24.92	3070	1169.67	0	0
$NaAl(OH)_4$	42.41	0.90	High	42.41		0
total	4687.99	100			3476.74	100

4.3. Precipitation with $CaCl_2$

In order to study the solubility of $CaCl_2$ using PHREEQC, data on this compound had to be incorporated since it is not in the database [47]. A value of $-1 \cdot 10^1$ mol/L is found as the water solubility output value. A negative data value indicates that $CaCl_2$ does not precipitate in these conditions.

It is also known that the ions are completely dissolved because the moles of Ca^{2+} correspond to the same value of solubility and the moles of Cl^- are double, this is given by the reaction in equilibrium.

$$CaCl_2 \rightleftarrows Ca^{2+} + 2Cl^-$$

Table 8 Input and output data for $CaCl_2$ in PHREEQC.

```
SOLUTION 1
    temp      25
    pH        7
    pe        4
    redox     pe
    units     mmol/kgw
    density   1
    -water    1 # kg

EQUILIBRIUM_PHASES 1
    CaCl2     0 10

PHASES
CaCl2
    CaCl2 = Ca+2 + 2Cl-
    log_k     100
END
```

```
-------------------------------Phase assemblage--------------------------------

                                                        Moles in assemblage
Phase               SI  log IAP  log K(T, P)   Initial       Final       Delta

CaCl2          -92.29     7.71    100.00    1.000e+01           0  -1.000e+01

-----------------------------Solution composition------------------------------

      Elements           Molality       Moles

      Ca                1.000e+01   1.000e+01
      Cl                2.000e+01   2.000e+01
```

4.3.1. Proposed reactions

The thermodynamic study of the following reactions has been carried out if $CaCl_2$ is added to the input current.

The main reaction of interest is the reaction (21) since it produces CaF_2. Previous studies on CaF_2 precipitation using $CaCl_2$ have also been conducted, and have shown that the rate of Ca addition controls the rate of precipitation [48].

The (21) and (22)reaction are considered as main reactions and the (23),(24),(25),(26) and (27) reaction are considered as a secondary reaction since $NaAl(OH)_4$ reacts with $CaCl_2$.

$$NaF + CaCl_2 \rightarrow NaCl + CaF_2 \quad (21)$$

$$NaOH + CaCl_2 \rightarrow NaCl + Ca(OH)_2 \quad (22)$$

$$NaAl(OH)_4 + CaCl_2 \rightarrow NaAlCl_4 + Ca(OH)_2 \quad (23)$$

$$NaAl(OH)_4 + CaCl_2 \rightarrow Al(OH)_3 + Ca(OH)_2 + NaCl \quad (24)$$

$$NaAl(OH)_4 + CaCl_2 + O_2 \rightarrow NaOH + Al_2O_3 + Ca(OH)_2 + Cl_2 \quad (25)$$

$$NaAl(OH)_4 + CaCl_2 \rightarrow AlCl_3 + NaOH + Ca(OH)_2 \quad (26)$$

$$NaAl(OH)_4 + CaCl_2 \rightarrow NaCl + AlCl_3 + Ca(OH)_2 \quad (27)$$

The same method of the study explained for the case of $CaCO_3$ has been followed, using HSC Chemistry for the temperature range between 0 and 90°C. Figure 15 shows the results obtained

from the thermodynamic study. For each reaction only the one with the lowest Gibbs energy value is shown, being the most likely thermodynamically. As it can be seen in the graph, reaction (23), (25), (26), and (27), in blue, grey, green and dark blue, do not occur spontaneously as they do not have ΔG values below 0, as well as the equilibrium constant of the reactions, do not support the reaction in the given directions due to the solution content.

The reaction that produces CaF_2 is the most thermodynamically favorable (reaction (21) in light blue color).

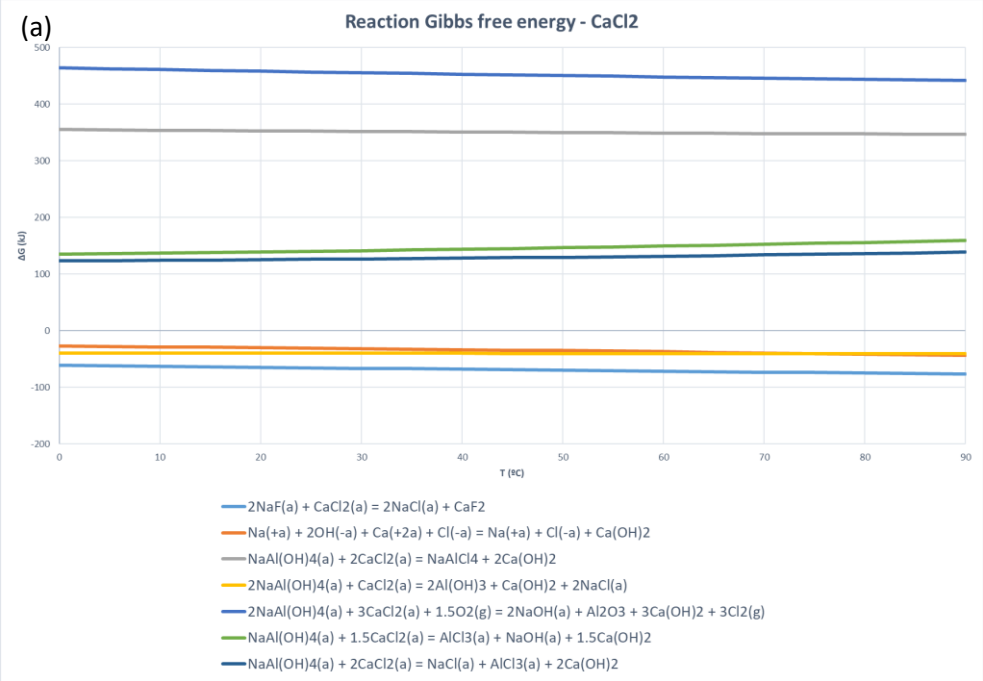

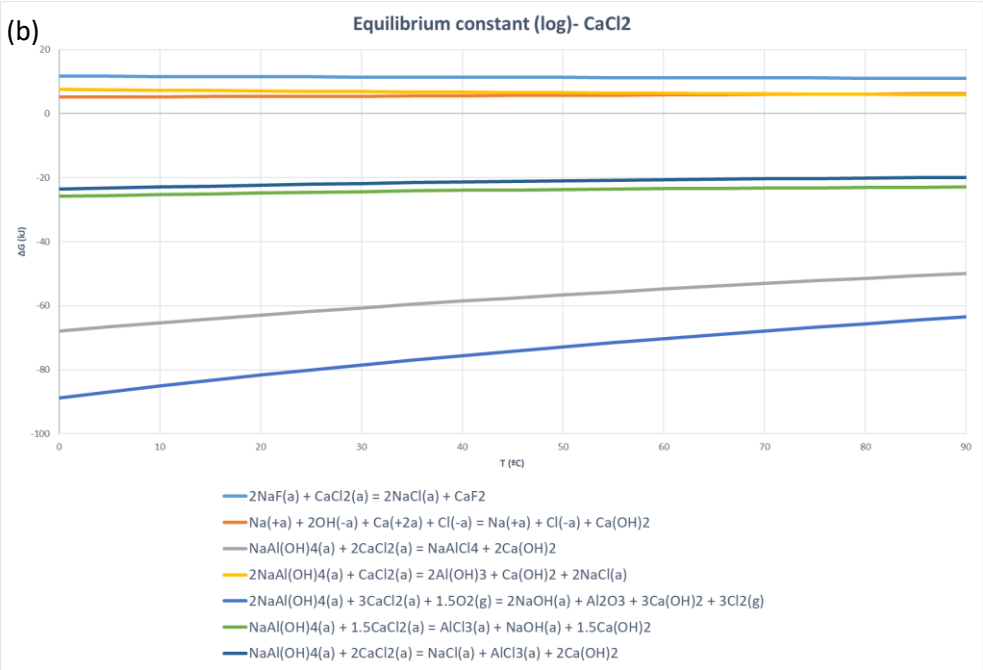

Figure 15 (a) Gibbs free energy and (b) reaction equilibrium constant changes by the temperature of possible reactions with $CaCl_2$.

If the study of the equilibrium constant is focused, reaction (21) is also the one with the highest logK values. This gives hopeful results for the production of CaF_2 with $CaCl_2$.

4.3.2. Equilibrium composition

From the input data of Table 1 and using the Equilibrium Composition Model (GEM) of HSC Chemistry, adding $CaCl_2$ the equilibrium composition obtained has been studied. As mentioned above, high values have been used to simulate an industrial process (for 10,000h). Although the final percentage values obtained do not change for a small laboratory-scale system as a similar multiplication was applied to all species.

As shown in Figure 16, CaF_2 production is stagnant before the introduction of 30 kmol of $CaCl_2$. When CaCl2 is added to the input current, it initially decreases Na(+a), F(-a) and NaF. Although these three compounds are present in less quantity, the amount of NaCl and CaF_2 increases. The development of reaction (21) is observed with the decrease of NaF when $CaCl_2$ is introduced and the increase of NaCl and CaF_2.

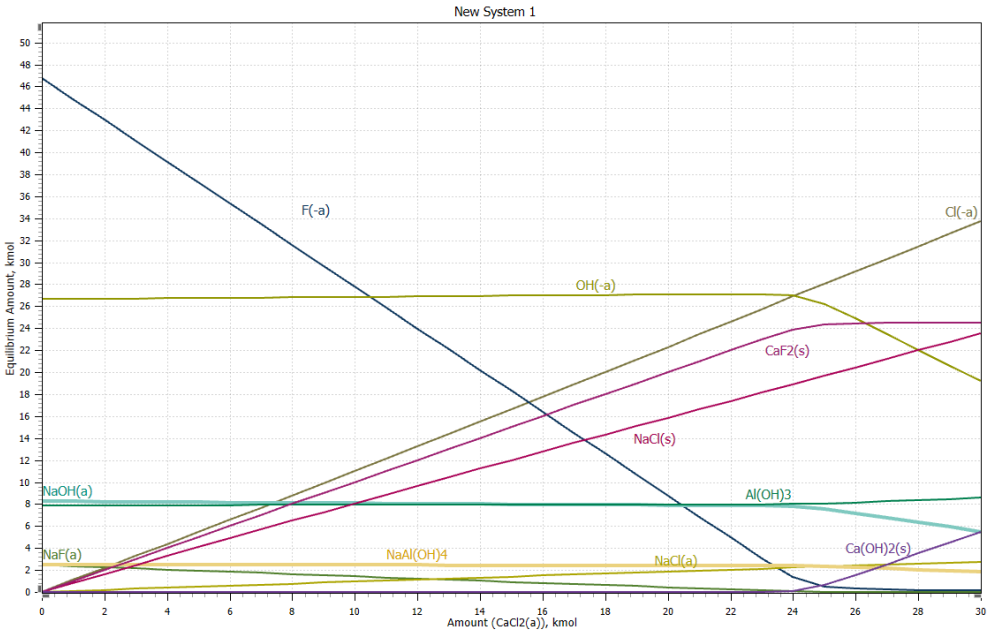

Figure 16 Evolution of the equilibrium amount of each component according to the added amount of $CaCl_2$.

The water and Na(+a) components have also been excluded from these graphs in order to observe the results more clearly, as they present high values of composition in equilibrium. The quantity of water is not modified by the introduction of $CaCl_2$. In contrast, the amount of Na(+a) in equilibrium is reduced due to the formation of NaCl salt.

Figure 17 shows the solids obtained in this precipitation study. CaF_2, NaCl, $Al(OH)_3$, $NaAl(OH)_4$ and $Ca(OH)_2$ have been found as solid compounds. Later, the purity of the obtained solid was calculated according to the theoretical equilibrium results.

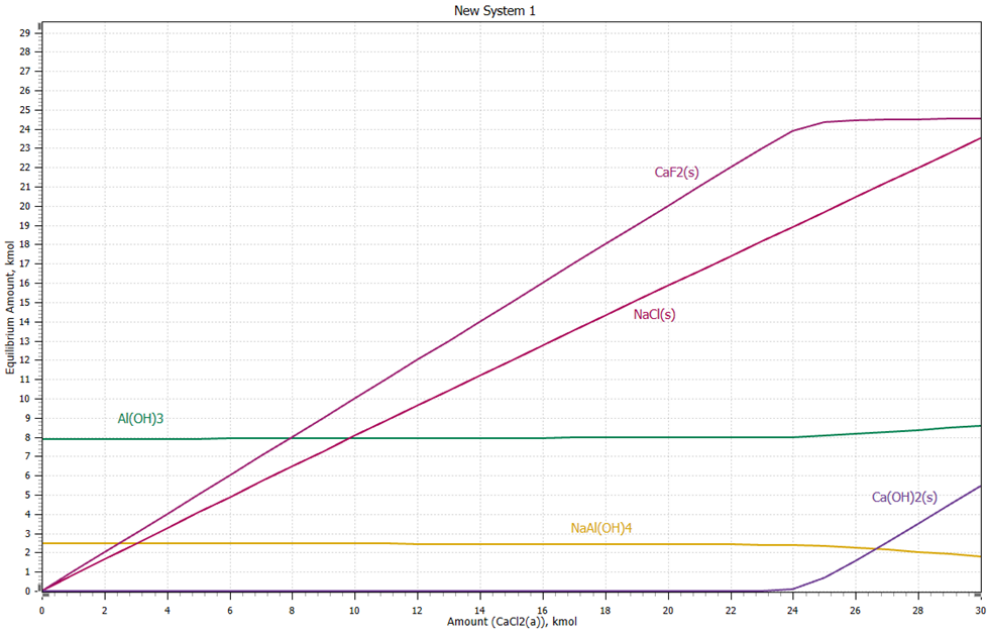

Figure 17 Evolution of solids compounds according to the added amount of $CaCl_2$.

This study has also been carried out on the compositions in equilibrium by varying the temperature and adding water to the system. These modifications have not caused changes in the results obtained with the composition in solid equilibrium, as shown in Figure 18 and Figure 19. The similar result had already been obtained in the case of precipitation with $CaCO_3$.

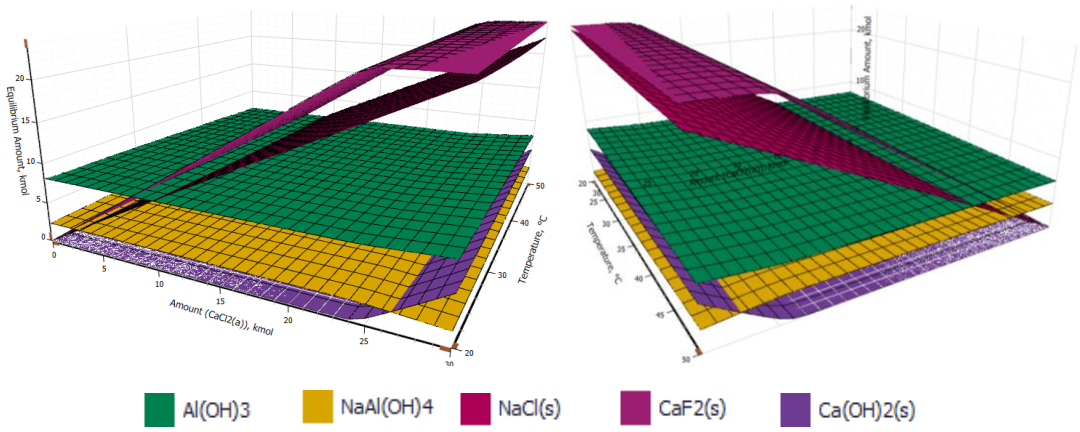

Figure 18 Evolution of solid components according to the added amount of $CaCl_2$ and temperature.

In Appendix B, the graphs of the evolution for the rest of the compounds studied can be observed. None of the compounds are modified by changing the temperature or adding water to the system.

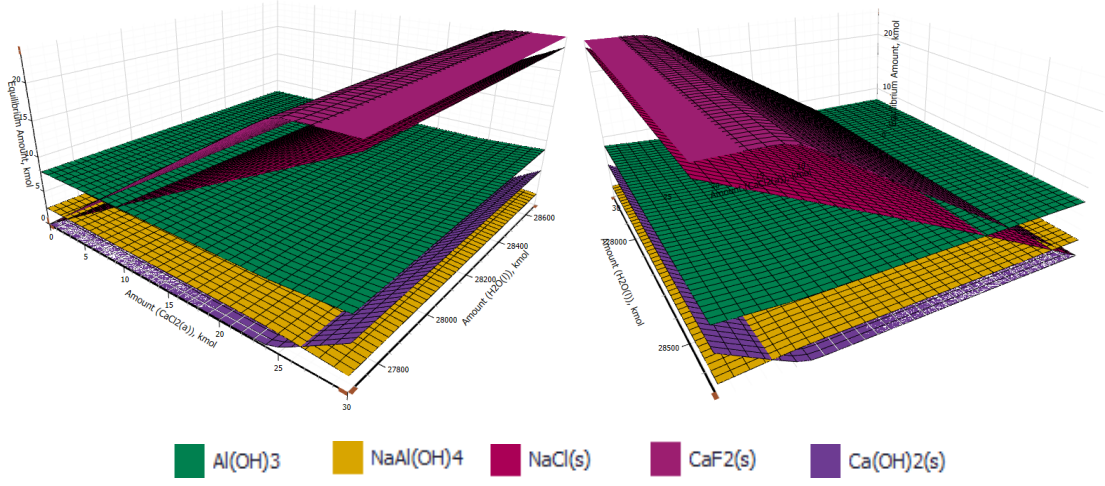

Figure 19 Evolution of solid components according to the added amount of $CaCl_2$ and water.

In the case of precipitation with $CaCl_2$, following the criteria explained above, it is considered that the production of CaF_2 reaches its maximum value in step 28 with the introduction of 27 kmol of $CaCl_2$.

Table 9 shows the composition of the sample after step 28.

Table 9 Composition of step 28 with the addtion of 27kmol $CaCl_2$.

	Equilibrium Amount	*Equilibrium Composition*
Species	kmol	mol fraction
NaF(a)	0.011467	4.09E-07
CaCl2(a)	6.75E-08	2.41E-12
Na(+a)	249.01	0.008871
Cl(-a)	30.31	0.00108
Ca(+2a)	8.28E-05	2.95E-09
F(-a)	0.235	8.36E-06
H2O(l)	27700	0.987
NaAl(OH)4(a)	0.038037	1.36E-06
NaOH(a)	6.74	0.00024
Al(OH)3	8.26	0.000294
NaAlCl4	7.95E-74	2.83E-78
Al(+3a)	8.09E-29	2.88E-33
OH(-a)	23.46	0.000836
NaCl(a)	2.48	8.84E-05
Ca(OH)2(ia)	2.49E-07	8.86E-12
NaAl(OH)4	2.136951	7.61E-05
Al(OH)3(a)	1.21E-08	4.32E-13
AlCl3(a)	1.46E-33	5.2E-38
AlCl3(s)	1.04E-75	3.69E-80
CaCl2(s)	3.64E-17	1.3E-21
NaCl(s)	21.20996	0.000756
CaF2(s)	**24.47699**	0.000872
Ca(OH)2(s)	2.52	8.99E-05
NaOH(s)	7.6E-05	2.71E-09

The pH of the water phase has been calculated using the composition of the following components: NaF, $CaCl_2$, $NaAl(OH)_4$, NaOH, NaCl, $Ca(OH)_2$, $Al(OH)_3$, $AlCl_3$. Appendix C shows the data used to calculate this pH. A pH value of 12.08 has been obtained for the solution.

The purity of the solid obtained has been calculated from the solid compounds determined in the thermodynamic study. As shown in Table 10 a purity of 45.14% CaF_2 has been reached.

Table 10 Purity data obtained for precipitation with $CaCl_2$.

Species	***Purity (%)***
Al(OH)3	15.21
NaAlCl4	0.00
NaAl(OH)4	5.96
AlCl3(s)	0.00
CaCl2(s)	0.00
NaCl(s)	29.28
CaF2(s)	45.14
Ca(OH)2(s)	4.42

The Heat and Material Balances Module (Bal) was used to determine the temperature of the products. The value obtained is close to the input value, 25.4°C.

Table 11 Result obtained from the Bal module.

Temperature of products = 25.4 °C (when Heat Balance = 0)

BALANCE	Amount kmol	Amount kg	Amount Nm^3	Heat Content kWh	Total H kWh	EXERGY kWh
IN1	2.81E+04	5.11E+05	544.2	0.00	-2.24E+06	6324
OUT1	2.81E+04	5.11E+05	502.3	0.00	-2.24E+06	6134
BALANCE	5.4	-111.0	-41.9	0.00	133.9	-191

4.3.3. Washing stage

It is proposed to carry out a washing stage of the solution obtained with the aim of reaching a higher purity of CaF_2. It is calculated that 345 L of water should be required for the total amount of 4233.62 kg of precipitate to dissolve NaCl and $NaAl(OH)_4$. In this case, CaF_2 purity can reach to 69.71% as shown in Table 12.

Table 12 Characteristics of washing process after precipitation with $CaCl_2$.

Species	*Initial amount (kg)*	*Purity (%)*	*Solubility (g/L)*[46]	*Solubilized (kg)*	*Insoluble(kg)*	*Purity (%)*
				Adding 345 L of water		
Al(OH)3	643.92	15.21	Insoluble	0	643.92	23.49
NaAlCl4	0.00	0.00			0	0
NaAl(OH)4	252.16	5.96	High	252.16	0	0
AlCl3(s)	0.00	0.00			0	0
CaCl2(s)	0.00	0.00			0	0
NaCl(s)	1239.57	29.28	3600	1242	0	0
CaF2(s)	1911.04	45.14	0.17	0.059	1910.98	69.71
Ca(OH)2(s)	186.93	4.42	1.59	0.547	186.38	6.80
NaOH(s)	0.00	0.00				

4.4. Precipitation with $Ca(OH)_2$

The solubility of $Ca(OH)_2$ in water has been studied with PHREEQC. In this case, the data of the compound [47] had to be introduced because it was not in the database.

In the output data, a delta value of $-1.903 \cdot 10^{-2}$ mol/L has been obtained, indicating its solubility.

$$Ca(OH)_2 \rightleftarrows Ca^{2+} + OH^-$$

Table 13 Input and output data for $Ca(OH)_2$ in PHREEQC.

```
SOLUTION 1
    temp      25
    pH        7
    pe        4
    redox     pe
    units     mmol/kgw
    density   1
    -water    1 # kg

EQUILIBRIUM_PHASES 1
    CalciumHydroxide 0 10

PHASES
CalciumHydroxide
Ca(OH)2=Ca+2 + 2OH-
log_k       -5.26
END
```

```
-------------------------------Phase assemblage--------------------------------

                                                                Moles in assemblage
Phase              SI  log IAP  log K(T, P)   Initial       Final       Delta

CalciumHydroxide   0.00    -5.26     -5.26    1.000e+01   9.981e+00  -1.903e-02

-----------------------------Solution composition------------------------------

      Elements           Molality       Moles

      Ca                1.903e-02   1.903e-02
```

4.4.1. Proposed reactions

For the study of precipitation with $Ca(OH)_2$, the following reactions have been proposed. Equation (28) is the reaction of interest given that CaF_2 is obtained as a precipitate.

Reactions (28), (29), (30), (31), (32) and (33) are considered as main reactions and reaction (34) is considered as a possible side reaction.

$$NaF + Ca(OH)_2 \rightarrow CaF_2 + NaOH \quad (28)$$

$$Ca(OH)_{2(ia)} \rightarrow Ca(OH)_2 \quad (29)$$

$$NaOH + Ca(OH)_2 \rightarrow NaOH + CaO + H_2O \quad (30)$$

$$NaOH + Ca(OH)_2 \rightarrow NaOH + CaO + Ca(OH)_2 + H_2O \quad (31)$$

$$NaOH + Ca(OH)_2 \rightarrow Ca(OH)_2 + Na_2O + H_2O \quad (32)$$

$$NaOH + Ca(OH)_2 \rightarrow NaOH + Ca(OH)_2 + Na_2O + H_2O \quad (33)$$

$$NaAl(OH)_4 + Ca(OH)_2 \rightarrow NaOH + Al(OH)_3 + CaO + H_2O \quad (34)$$

Using the reaction equations module of HSC Chemistry, the thermodynamic study of these reactions has been carried out for temperatures between 0 and 90°C.

Reaction (30), (32), (33) and (34) do not occur spontaneously thermodynamically since they do not present negative values of Gibbs free energy for any of the temperatures. In addition, at equilibrium, reagents are preferred to products because they have negative logarithmic values of equilibrium constant. The most favourable reaction is the reaction that CaF_2 is obtained as a precipitate (reaction(28)) as presented in Figure 20.

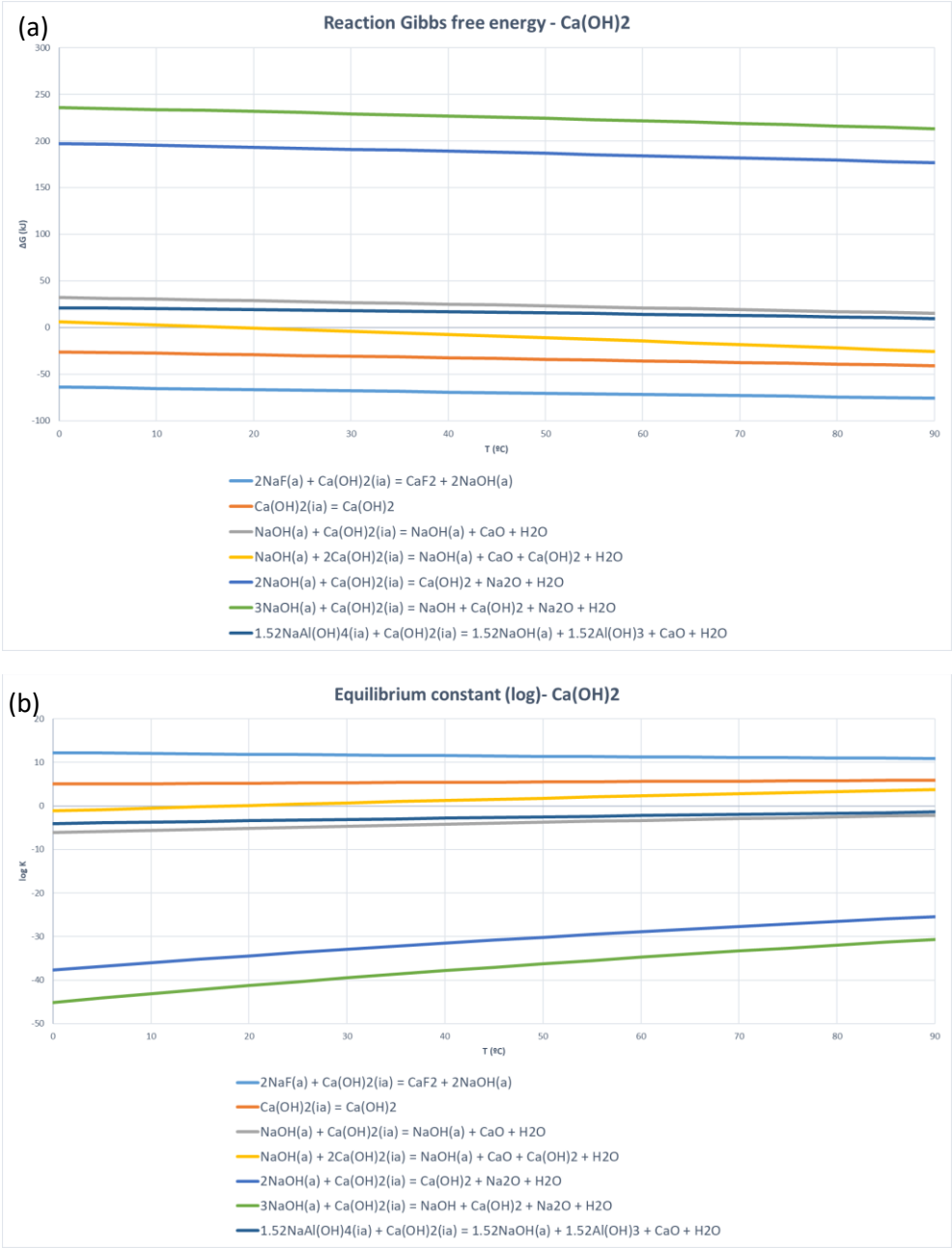

Figure 20 (a) Gibbs free energy and (b) reaction equilibrium constant changes by the temperature of possible reactions with $Ca(OH)_2$.

In the case of equilibrium constant (Figure 20 b), the reaction that produces CaF_2 as a precipitate is the one that has higher values of this parameter. This confirms the thermodynamic spontaneity of the reaction.

4.4.2. Equilibrium composition

The Equilibrium Composition Model (GEM) of HSC Chemistry has been used to study the equilibrium composition of precipitation with $Ca(OH)_2$. This study was carried out by simulating

an industrial process for 10,000h of input current. The results obtained can be taken to a laboratory scale due to the preservation of the study ratio.

This precipitation agent presents different characteristics to $CaCl_2$ and $CaCO_3$. CaF_2 generation does not reach a clear stagnation point, but the slope of the curve is reduced before step 40.

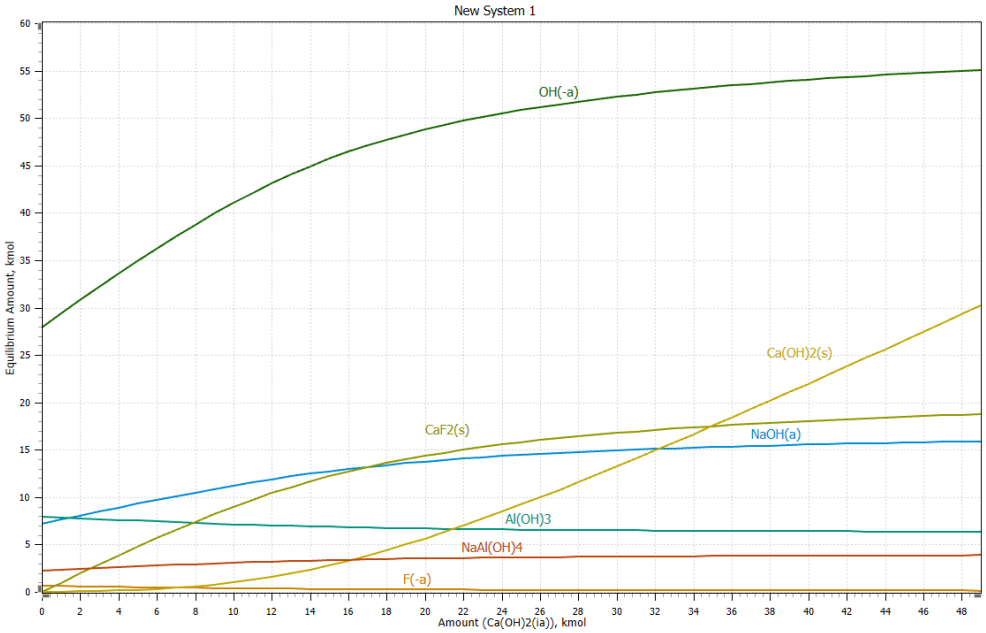

Figure 21 Evolution of the equilibrium amount of each component according to the added amount of $Ca(OH)_2$.

Another of the singularities is that in step 36, with the addition of 35 kmol of $Ca(OH)_2$, the solids species of CaF_2 and $Ca(OH)_2$ present the same equilibrium amount. From this point on, the quantity of $Ca(OH)_2$ is greater than the quantity of CaF_2. Thus, this indicates that even if $Ca(OH)_2$ continues to be added, the solid obtained will not contain a higher purity of CaF_2. One of the reasons for this is that the reaction (28) has stopped, possibly because there is no more NaF left to react with.

Figure 22 shows equilibrium composition for solids obtained in precipitation with $Ca(OH)_2$, commented previously.

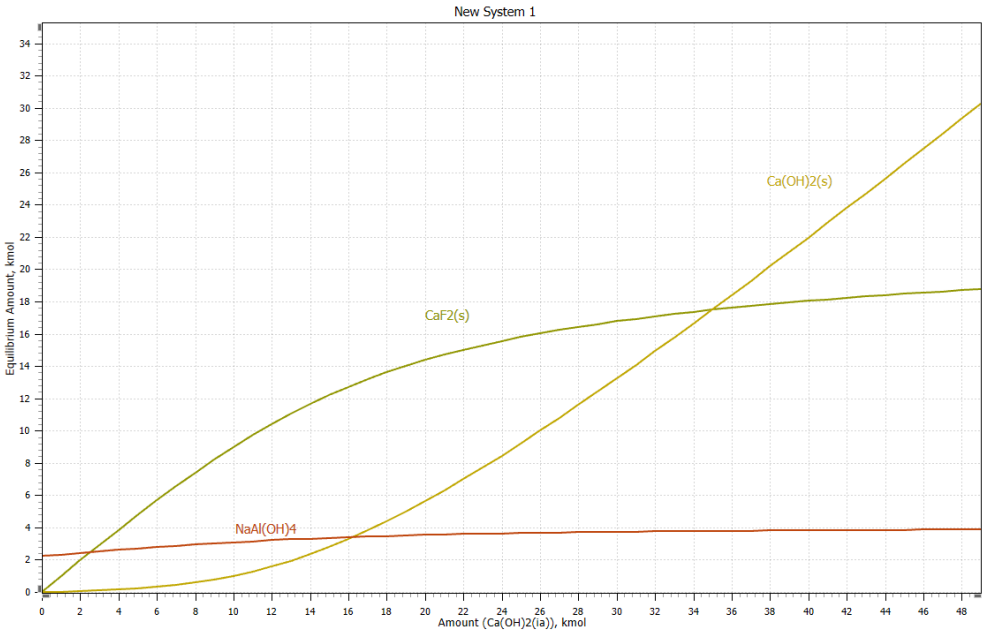

Figure 22 Evolution of solids compounds according to the added amount of $Ca(OH)_2$.

Similar results to the other precipitations have been obtained by realizing the three-dimensional study with the evaluation of the temperature and adding water to the system.

As it is observed in Figure 23 and Figure 24, the variation of temperature between 20 and 90°C and the addition of water up to 28100 kmol, does not cause changes in the obtained results. In this two figures NaF is shown as a solid by mistake, because this compound is in solution and not in solid form. This only modifies the evolution of this compound in these figures and not in the results.

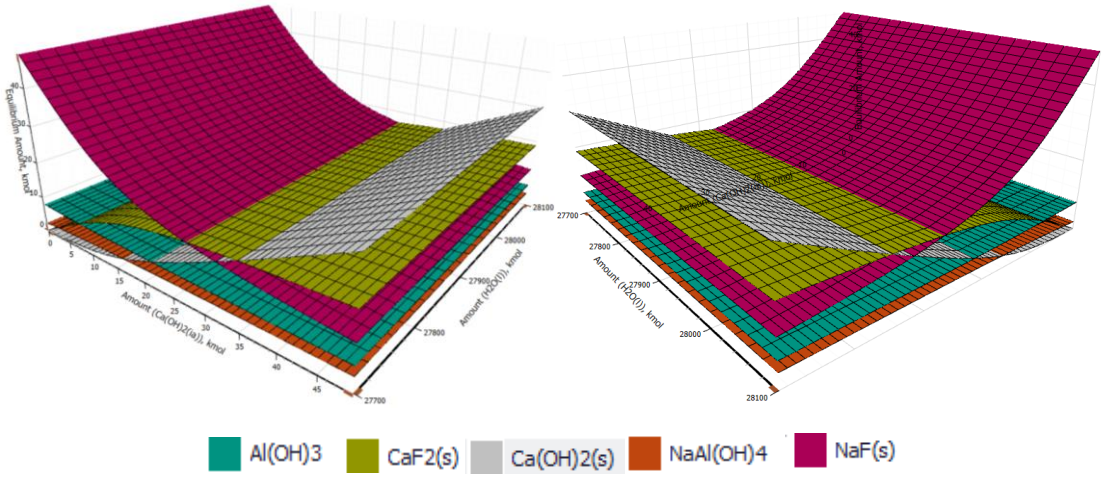

Figure 23 Evolution of components according to added amount of $Ca(OH)_2$ and water.

The evolution of the other compounds studied in this precipitation has not been modified either, as can be seen in the graphs in Appendix B.

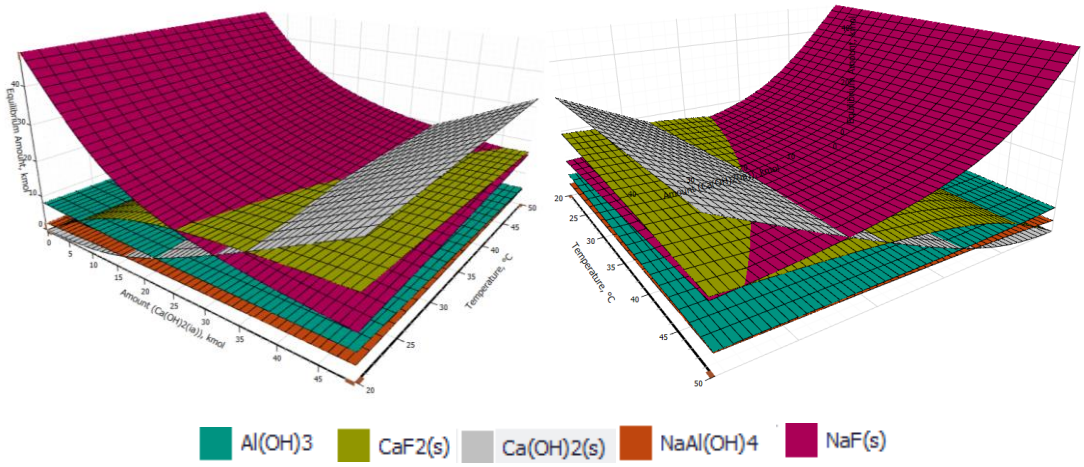

Figure 24 Evolution of solid components according to the added amount of $Ca(OH)_2$ and increase temperature.

If the criteria used in the previous precipitations is followed, where the highest production of CaF_2 is reached when its increment is less than 0.5 kmol, step 41 is selected. at this point, the equilibrium amount of $Ca(OH)_2$ will be greater than CaF_2, the intersection point of these two components is selected as an interesting point to study. Table 14 shows the concentrations of these two study points.

Table 14 Composition of step 36 and 41 with the of $Ca(OH)_2$.

	Equilibrium Amount		*Equilibrium Composition*	
	kmol		mol fraction	
Step	36	41	36	41
Ca(OH)2(ia) added	35	40	35	40
NaF(a)	8.33E-03	7.69E-03	2.97E-07	2.74E-07
Ca(OH)2(ia)	1.73E-06	2.16E-06	6.15E-11	7.71E-11
Na(+a)	2.48E+02	2.49E+02	8.85E-03	8.87E-03
Ca(+2a)	1.12E-04	1.36E-04	3.97E-09	4.84E-09
F(-a)	1.71E-01	1.57E-01	6.09E-06	5.60E-06
H2O(l)	2.77E+04	2.77E+04	9.87E-01	9.86E-01
NaAl(OH)4(a)	6.73E-02	6.80E-02	2.40E-06	2.42E-06
NaOH(a)	1.53E+01	1.55E+01	5.44E-04	5.54E-04
Al(OH)3	6.45E+00	6.41E+00	2.30E-04	2.28E-04
Al(+3a)	5.40E-30	5.14E-30	1.92E-34	1.83E-34
OH(-a)	5.33E+01	5.41E+01	1.90E-03	1.93E-03
CaF2(ia)	1.72E-12	1.78E-12	6.14E-17	6.33E-17
CaF2(s)	1.75E+01	1.80E+01	6.23E-04	6.42E-04
NaOH(s)	1.72E-04	1.75E-04	6.13E-09	6.24E-09
Ca(OH)2(s)	1.75E+01	2.20E+01	6.24E-04	7.82E-04
CaO(s)	1.33E-09	1.66E-09	4.73E-14	5.93E-14
Na2O(s)	2.99E-38	3.09E-38	1.06E-42	1.10E-42

NaAl(OH)4	3.78E+00	3.82E+00	1.35E-04	1.36E-04
Al(OH)3(a)	9.48E-09	9.42E-09	3.38E-13	3.35E-13
Al2O3(s)	6.58E-02	6.49E-02	2.34E-06	2.31E-06

Considering to equilibrium composition results, adding 40 kmol of $Ca(OH)_2$ gives a theoretical purity of 35.27% of CaF_2, as shown in Table 15.

Table 15 Purity obtained after the addition of 40 kmol of $Ca(OH)_2$.

Species	***Purity (%)***
Al(OH)3	12.52
CaF2(s)	35.27
NaOH(s)	0.00
Ca(OH)2(s)	40.75
CaO(s)	0.00
Na2O(s)	0.00
NaAl(OH)4	11.3
Al2O3(s)	0.17

For the pH calculation, the concentrations of the following species have been taken into account: NaF, $Ca(OH)_2$, $NaAl(OH)_4$, NaOH, CaF_2 and $Al(OH)_3$. A pH of 12.42 has been obtained, following the calculations shown in Appendix C.

An output current temperature of 25.4°C has been obtained using the Heat and Material Balances Module (Bal).

Table 16 Result obtained from the Bal module

Temperature of products = 25,4 °C (when Heat Balance = 0)

BALANCE	**Amount kmol**	**Amount kg**	**Amount Nm³**	**Heat Content kWh**	**Total H kWh**	**EXERGY kWh**
IN1	2.81E+04	5.11E+05	544.2	0.00	-2.24E+06	6725
OUT1	2.81E+04	5.11E+05	502.1	0.00	-2.24E+06	6484
BALANCE	12.9	0.000	-42.1	0.00	-4.16	-241

4.4.3. Washing stage

As already proposed in the previous precipitations, the study of a washing stage has been designed. In this case, performing this process is not effective because the impurities in the solid have a very low solubility value as shown In Table 17. This requires that a very high water amount values should be added.

Table 17 Solubility study of solid components.

Species	***Initial amount (kg)***	***Purity (%)***	***Solubility (g/L)*** [46]
Al(OH)3	499.92	12.52	insoluble
CaF2(s)	1408.34	35.27	0.17
NaOH(s)	0.01	0.00	
Ca(OH)2(s)	1627.19	40.75	1.59
CaO(s)	0.00	0.00	
Na2O(s)	0.00	0.00	
NaAl(OH)4	451.12	11.3	high
Al2O3(s)	6.62	0.17	insoluble
total	3993.20	100	

4.5. Comparison between precipitation agents

The reaction with the lowest ΔG has been selected to compare the results obtained for each precipitating agent. In all cases, the thermodynamically spontaneous reaction is the one that produces CaF_2 as a precipitate. Although, as shown in Figure 25 the precipitation with $Ca(OH)_2$ is the most thermodynamically favorable, it is not the one with the highest purity value in the solid obtained (Table 18). In addition, as explained in the following section, $Ca(OH)_2$ and $CaCO_3$ have solubility problems. Thus $Ca(OH)_2$ and specifically $CaCO_3$ are not a proper precipitation agent.

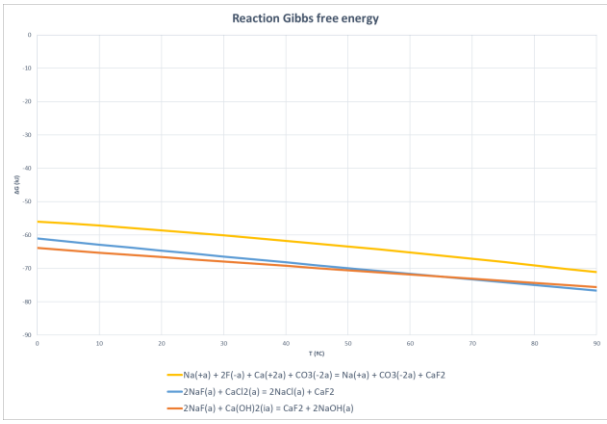

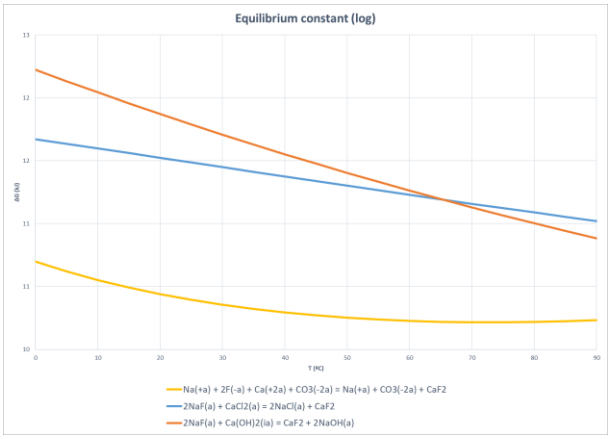

Figure 25 Gibbs free energy and evolution of equilibrium constant logarithm for each precipitating agent.

In terms of solid purity more favourable results have been obtained for the use of $CaCl_2$. On the other hand, no differences have been found concerning the quantity for the addition of the different precipitation agents. Also in all cases, the calculated pH values have been almost similar, between 12 and 12.5.

In the case of the ratio between the mole amounts of NaF and CaF_2, a low value is of interest since it would indicate a high production of CaF_2. On the contrary, in the ratio between NaF and the precipitating agent, a high value is of interest since it indicates that greater consumption of the NaF component with less addition of the precipitation agent (Table 18).

Table 18 Data collection for the different precipitations.

	Precipitation agent amount		*CaF2 purity*		*pH*	*Ratios*	
	kmol	kg	(%)			kmol NaF/kmolCaF_2	kmol NaF/kmol precipitating agent
			Before washing stage	After washing stage			
CaCO3	27	2702.3	40.7	54.9	12.20	2.0136	1.82
CaCl2	27	2996.6	45.1	69.7	12.08	2.0101	1.82
Ca(OH)2	40	2963.7	35.27	35.27	12.42	2.8131	1.41

It should be noted that these calculations have been made taking into account the criteria explained in chapter 4.2.2. as a final point of precipitation.

4.6. Experimental study

The thermodynamic calculations performed with HSC Chemistry have been tested in the laboratory. To prepare 50 mL of the initial artificial solution of NaOH, NaF and $NaAl(OH)_4$, the procedure explained in chapter 3 has been followed and the amounts shown in Table 19 have

been used. The amounts of the precipitating agents to be added were calculated from the ratio obtained between the amount of NaF present in the sample and the amount of precipitation agent to be added, shown in Table 18.

Table 19 Composition of the input sample to be prepared.

Solution to prepare:	*Amount (g)*
NaOH(a)	0.1478
NaF(a)	0.3391
$Al(OH)_3$	0.0814

Precipitating agent	*Amount (g)*	*Solubility (g/100ml)*[46]	*Amount of water needed (ml)*
$CaCl_2$ (a)	0.4919	74.5	
$Ca(OH)_2$ (a)	0.4865	0.173	281.2
$CaCO_3$ (a)	0.4436	0.0013	31684

The NaOH amount is calculated from the 0.0417 g needed to prepare $NaAl(OH)_4$ and the rest was the required NaOH in the sample.

It should be noted that the solubility of $Ca(OH)_2$ and $CaCO_3$ are very low (Table 19), and the calculated amounts of precipitating agents addition exceed the solubility limit. For example, in the case of $Ca(OH)_2$, only 0.0865 g could be dissolved but the required calculated amount is 0.4865 g. This may cause that not all the precipitation agent is dissolved and it can be present in the solid obtained, even if the agent should consume by the precipitation reactions. For this reason, it has been chosen to carry out some experiments with smaller quantities than those calculated.

In the case of $Ca(OH)_2$, precipitation with 41.56% of the required agent has been implemented that leads to obtain a solid with a weight of 0.2461 g.

As $CaCO_3$ presents less solubility value, it was decided to make two partial precipitations: using 22.7 and 67.8% of the calculated amount of precipitation agent.

Table 20 shows the obtained data; precipitation agent amounts, yields depending on F- and agent, etc. For the calculation of the yield from NaF and the precipitation agent, it has been assumed that all the solid obtained is CaF_2 assuming that only the precipitation reaction takes place. This fact is not verified and for this reason, it is obtained that the amount of NaF consumed

Precipitating agent	*Amount of agent added (g)*	*Relation between agent calculated and added (%)*	*pH*	*Solid amount obtained (g)*	*Theoretical solid amount from NaF (g)*	*Yield from NaF(%)*	*Theoretical solid amount from precipitation agent (g)*	*Yield from agent (%)*	*Amount of NaF consumed (g)*	*Amount of NaF in solution, unreacted (g)*
$Ca(OH)_2$ 1st	0.2022	41.56	14.0	0.2461	0.3155	77.98	0.2131	115.48	0.2646	0.0747
$CaCO_3$ 1st	0.1007	22.71	13.5	0.0729	0.3158	23.09	0.0786	92.82	0.0785	0.2613
$CaCO_3$ 2nd	0.3007	67.78	13.0	0.2480	0.3158	78.51	0.2369	315.56	13.9826	-13.6429

is higher than the one present in the initial sample and that the amount of NaF in the final aqueous solution is negative.

Table 20 Data obtained for partial precipitations.

Precipitating agent	*Amount of agent added (g)*	*Relation between agent calculated and added (%)*	*pH*	*Solid amount obtained (g)*	*Theoretical solid amount from NaF (g)*	*Yield from NaF(%)*	*Theoretical solid amount from precipitation agent (g)*	*Yield from agent (%)*	*Amount of NaF consumed (g)*	*Amount of NaF in solution, unreacted (g)*
$Ca(OH)_2$ 1st	0.2022	41.56	14.0	0.2461	0.3155	77.98	0.2131	115.48	0.2646	0.0747
$CaCO_3$ 1st	0.1007	22.71	13.5	0.0729	0.3158	23.09	0.0786	92.82	0.0785	0.2613
$CaCO_3$ 2nd	0.3007	67.78	13.0	0.2480	0.3158	78.51	0.2369	315.56	13.9826	-13.6429

Not considering the solubility values, the precipitation reactions for the three precipitation agents have been carried out in triplicate with the calculated quantity values. The values obtained are in

Table 21.

Precipitation agent	*Amount of agent added (g)*	*Final pH solution*	*Solid amount obtained (g)*	*Theoretical solid amount from NaF (g)*	*Yield from NaF(%)*	*Theoretical solid amount from precipitation agent (g)*	*Yield from agent (%)*	*Amount of NaF consumed (g)*	*Amount of NaF in solution, unreacted (g)*
$CaCl_2$	0.4855	13	0.2348 ±0.0546	0.3153	74.5	0.3416	68.7	0.2526	0.0864
$Ca(OH)_2$	0.4259	14	0.5224 ±0.0219		165.7	0.4488	116.4	0.5619	-0.2227
$CaCO_3$	0.4438	13.5	0.3944 ±0.0032		125.1	0.3462	113.9	0.4242	-0.0850

Table 21 Data obtained in the precipitations.

Precipitation agent	*Amount of agent added (g)*	*Final pH solution*	*Solid amount obtained (g)*	*Theoretical solid amount from NaF (g)*	*Yield from NaF(%)*	*Theoretical solid amount from precipitation agent (g)*	*Yield from agent (%)*	*Amount of NaF consumed (g)*	*Amount of NaF in solution, unreacted (g)*
$CaCl_2$	0.4855	13	0.2348 ±0.0546	0.3153	74.5	0.3416	68.7	0.2526	0.0864
$Ca(OH)_2$	0.4259	14	0.5224 ±0.0219		165.7	0.4488	116.4	0.5619	-0.2227
$CaCO_3$	0.4438	13.5	0.3944 ±0.0032		125.1	0.3462	113.9	0.4242	-0.0850

The pH values have been measured every 15 min, but no changes have been found in any of the samples during the precipitation process. The pH value was only changed initially when the precipitation agent was added. After this addition, the pH value remains constant.

For the calculation with the data obtained in these reactions, it has also been considered that all the solid is CaF_2. Yield values greater than 100% have been obtained, which indicates that not all the solid corresponds to the CaF_2 compound since not only the precipitation reaction of this is produced.

A precipitation experiment of a real SPL sample was also performed. The chemical composition of this sample is shown in Table 22. Calcium chloride has been chosen as the precipitation agent for this reaction. The amount of this agent to be added has been calculated following stoichiometric calculations assuming that all the fluoride present in the sample reacts with $CaCl_2$. The volume of the sample used has been 435 mL.

Table 22 ICP-MS results of the real sample SPL

L/S (liquid/solid ratio) =2l/1000 g

Parameter	***SPL-1-1L(mg/L)***
Arsenic	0,059
Barium	0,0059
Cadmium	<0,0002
full chrome	0,087
Copper	0,066
Mercury	<0,0001
Molybdenum	0,12
Nickel	0,015
Lead	0,014
Antimony	0,0050
Selenium	0,0041
Zinc	0,053
Chlorides	1
Fluorides	**1,67**
Sulfates	<20

In this case, the initial pH of the sample was 14 and was not modified by the addition of the precipitating agent. Table 23 shows the data obtained for this precipitation. In this case, the yields are even higher than in the previous cases due to the presence of impurities in the solid obtained.

Table 23 Data obtained in real sample SPL precipitation.

Precipitating agent	*Amount of F in sample (g)*	*Initial pH*	*Amount of agent added (g)*	*Final pH*	*Solid amount obtained (g)*	*Theoretical solid amount from NaF (g)*	*Yield from NaF(%)*	*Theoretical solid amount from precipitation agent (g)*	*Yield from agent (%)*	*Amount of NaF consumed (g)*	*Amount of NaF in solution, unreacted (g)*
CaCl2	0.000726	14	0.00213	14	0.00301	0.00068	445.7	0.00150	200.77	0.003238	-0.00251

In relation to the visual aspect of the precipitates obtained, in the precipitates prepared with the synthesized sample, the solid obtained has been a white powder. On the other hand, in the precipitation made with the real sample, a brown colored precipitate has been obtained, due to the impurities present in this sample. Figure 26 shows the visual aspects of the samples.

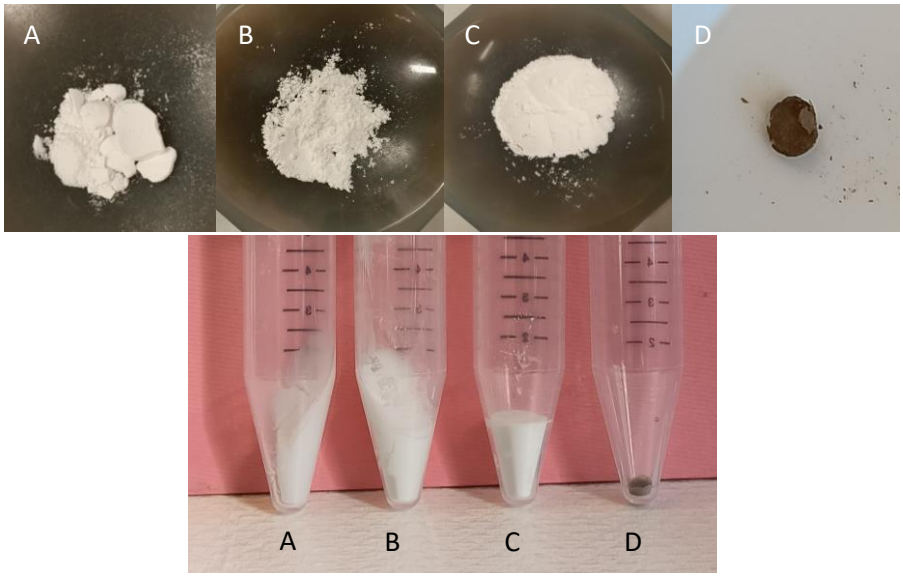

Figure 26 Appearance of the solids obtained from (a) $CaCl_2$, (b) $Ca(OH)_2$, (c) $CaCO_3$, and (d) real SPL with $CaCl_2$.

To study the composition of the precipitates, FTIR spectrums have been carried out, shown in Figure 27.

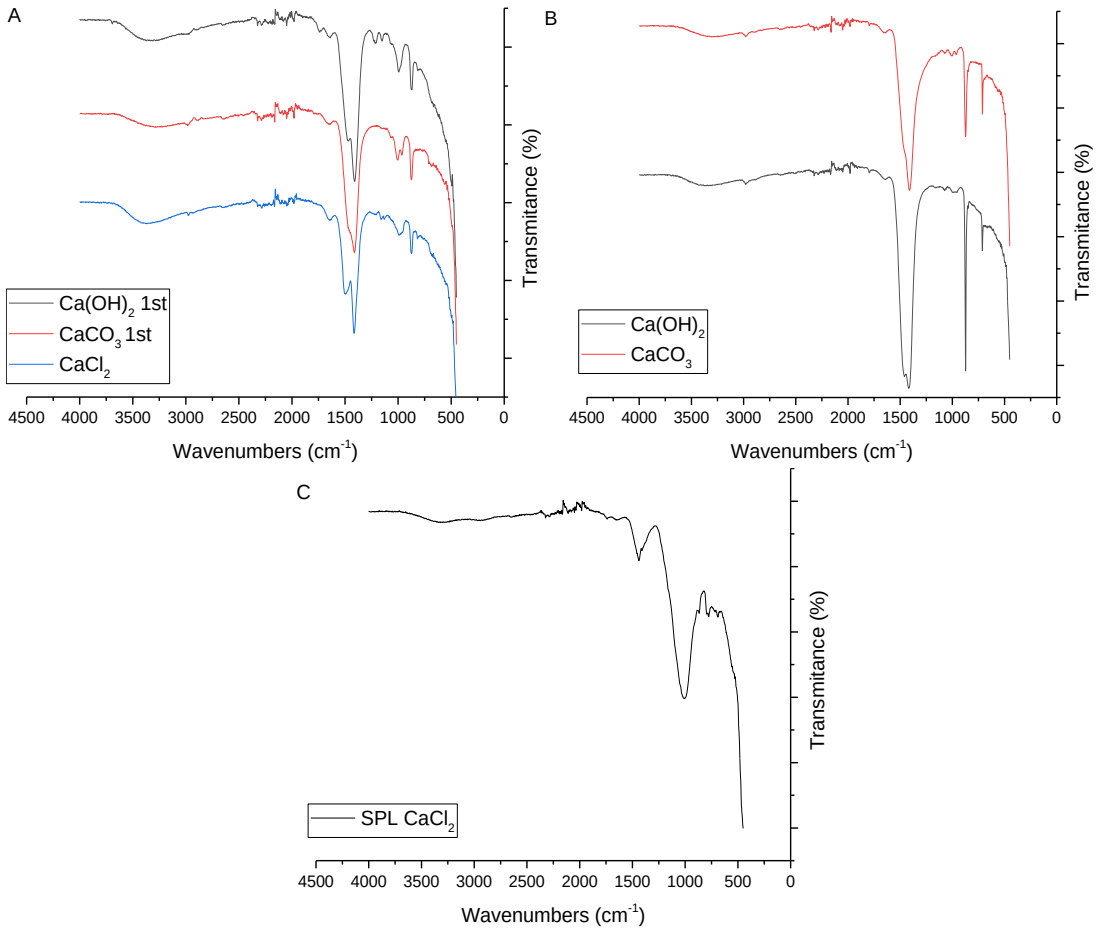

Figure 27 FTIR spectrum of precipitated samples.

The spectrum of pure CaF_2 has no peaks since it is a low index material and does not have OH absorption, as it can be seen in Figure 28. In this case, if the solid samples obtained are studied, not only CaF_2 is present.

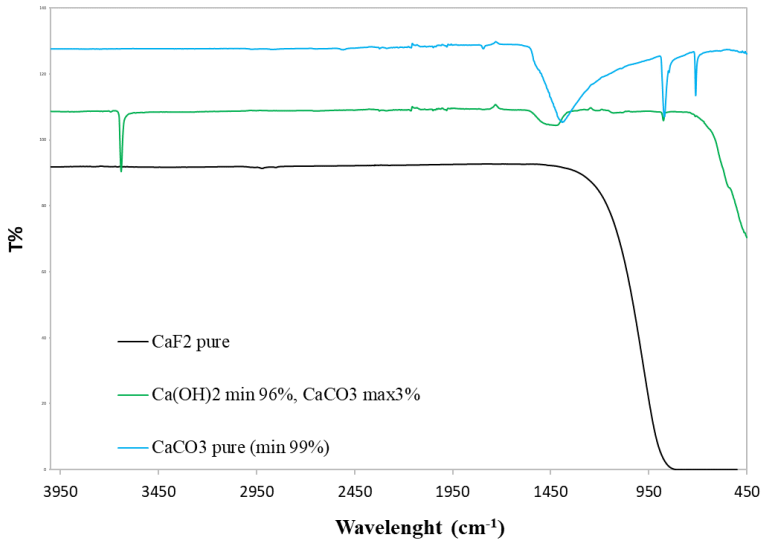

Figure 28 FTIR spectrum for pure chemicals.

The spectra of solid samples collected in graph B of Figure 27, corresponding to the precipitation of $Ca(OH)_2$ and $CaCO_3$ are similar. These two spectra correspond to $CaCO_3$ compounds as the peaks at around 1450, 1000 and 850 cm^{-1} belong to different vibration modes C-O of carbonate groups CO_3^{2-} [49].

The sample of Figure 27 A prepared with $CaCO_3$, also corresponds perfectly to the spectrum of $CaCO_3$.The precipitates obtained using $Ca(OH)_2$ contain $CaCO_3$ because the chemical agent used has a 3% impurity of $CaCO_3$. Since the solubility of $Ca(CO)_3$ is limited (0.013 g/L at 25°C), the impurity amount in the precipitation agent exceeds the solubility limit the experimental condition. In relation to the real sample prepared with $CaCl_2$, graph C, it is not related to any of the spectra consulted. This may be due to the presence of impurities in the sample.

The XRD patterns of the precipitates are shown in Figure 29 to determine the crystalline structure. It is clear that in the pattern of samples obtained by precipitation from artificial solution, the face centered cubic crystal structure calcium fluoride was found (PDF Card No:01-087-0971).

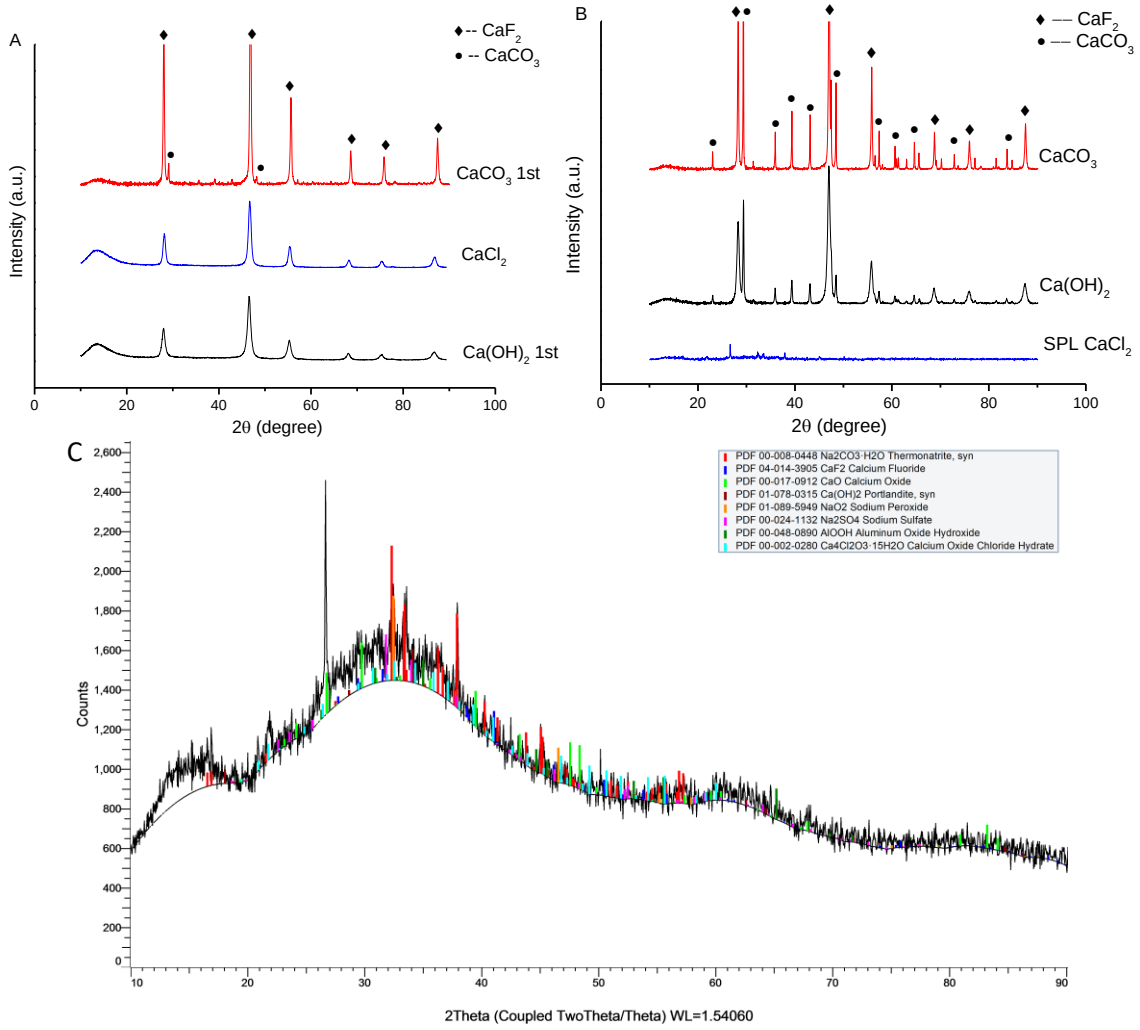

Figure 29 XRD patterns of precipitated samples.

In the samples prepared with $CaCO_3$ this compound is also found, both in the partial precipitation ($CaCO_3$ 1st, graphs A) and in the precipitation made with the amount of $CaCO_3$ ($CaCO_3$, graphs B) calculated. This may be due to the low solubility of this compound in water which prevents all the precipitation agents added with NaF to react.

One of the singular aspects is the presence of $CaCO_3$ in the samples prepared with $Ca(OH)_2$ ($Ca(OH)_2$, graphs B). This carbonate present in the XRD standard could have been obtained by contact with CO_2 or because the chemical reagent used ($Ca(OH)_2$) is not completely pure and has a maximum impurity of 3% $CaCO_3$.

XRD pattern of the artificial sample precipitated with $CaCl_2$ ($CaCl_2$, graphs A) shows that the precipitate contains only CaF_2 as a crystal structure. For this reason, this precipitation agent has been chosen as the most suitable one and it is with this agent that the precipitation of the real sample has been carried out.

The real sample (SPL $CaCl_2$, Graphs C) shows a pattern with many peaks. This is because the sample obtained contains impurities and was too small to be determined with XRD. The crystalline structure CaF_2 (PDF Card No: 04-014-3905) was detected in the pattern of this precipitate. Impurities were also detected as $Na_2CO_3 \cdot H_2O$ (PDF Card No: 00-008-0448), NaO (PDF Card No: 01-089-5949), CaO (PDF Card No: 00-017-0912), Na_2SO_4 (PDF Card No: 00-024-1132), $Ca_4Cl_2O_3 \cdot 15H_2O$ (PDF Card No: 00-002-0280), AlOOH (PDF Card No: 00-048-0890) and $Ca(OH)_2$ (PDF Card No: 01-078-0315) due to the initial composition of the real sample containing chlorides, sulfates and fluorides as main components.

5

CONCLUSIONS

Nowadays, fluorite (CaF_2) is one of the critical raw materials that presents risks of shortage for the EU. On the other hand, Spent Pot Lining (SPL) is a hazardous waste due to its content in fluorides and cyanides. Precipitation is considered a simple and cost-efficient method for removing fluoride from aqueous streams producing a valuable product. In this work, CaF_2 precipitation has been proposed for fluoride recovery from SPL recycling process solution by adding salts such as calcium carbonate, calcium chloride, and calcium hydroxide.

The thermodynamics of CaF_2 precipitation and the secondary reactions of water from the SPL recycling process were investigated. Using the HSC Chemistry software it was observed that there is no difference in the amount of each precipitation agent to be added and that the final pH value is similar in all cases, between 12-12.5. Theoretical calculations reveal that high purity CaF_2 can only be obtained with low recovery efficiency due to possible coprecipitation reactions. Among the three precipitation agents studied, it has been found that the one with higher purity values in thermodynamic calculations is $CaCl_2$.

Subsequent experimental investigations show the problems of solubilities limited by the precipitation agents used in the case of $Ca(OH)_2$ and $CaCO_3$.The generation of a solid composed of CaF_2 has been verified in all samples with the experimental study. By means of the characterization techniques used, FTIR and XRD, impurities have been observed in the real sample of SPL treated with $CaCl_2$ and it has been verified that the purity of the final product obtained by $Ca(OH)_2$ is affected by the impurity level of this agent used.

During the development of this work certain limitations have been found, like possible restrictions in the database of the softwares used or that the results of the thermodynamic calculations do not provide kinetic information or data on the reaction rate.

In order to verify these results experimentally and check the impurities contained in the solid, it is proposed to study the purity of the precipitate by inductively coupled plasma optical emission or mass spectrometer (ICP-OES or ICP-MS) analysis and the fluoride concentration by Ion chromatography. It is suggested as future studies to make more precipitations with real samples with the different precipitation agents. It is recommended to use a purer chemical agent or one containing soluble chemical components in the area of study, to increase the purity in the case of precipitation with $Ca(OH)_2$. Additionally, the study of the reaction time necessary to obtain the precipitate would be another important parameter for this process to be feasible on an industrial scale.

Based on the concept of the circular economy, the results present a reliable and environmentally friendly process where the waste from aluminium production is used. Besides, the research

indicates that the process could also be applied for the treatment of wastewater with a high concentration of fluorine. The resulting product has a high economic value and could be applied in the aluminium smelting industry. Therefore, the process has a wide and promising application perspective within the industry.

6

BIBLIOGRAPHY

[1] British Geological Survey, World Mineral Production 2014-2018, 2020. https://www.bgs.ac.uk/downloads/start.cfm?id=3512.

[2] The International Aluminium Institute, World Aluminium — Primary Aluminium Production, (2020). http://www.world-aluminium.org/statistics/primary-aluminium-production/#data (accessed April 19, 2020).

[3] N.I. Poulimenou, I. Giannopoulou, D. Panias, Use of ionic liquids as innovative solvents in primary aluminum production, Mater. Manuf. Process. 30 (2015) 1403–1407. https://doi.org/10.1080/10426914.2014.994762.

[4] Ecofys, Fraunhofer ISI, OKO-Institut e.V, Methodology for the free allocation of emission allowances in the EU ETS post 2012 Sector report for the aluminium industry, (2012). http://www.ecofys.com/files/files/091102_lime.pdf.

[5] G. Holywell, R. Breault, An overview of useful methods to treat, recover, or recycle spent potlining, Jom. 65 (2013) 1441–1451. https://doi.org/10.1007/s11837-013-0769-y.

[6] D. Brough, H. Jouhara, The Aluminium Industry: A Review on State-of-the-Art Technologies, Environmental Impacts and Possibilities for Waste Heat Recovery, Int. J. Thermofluids. 2 (2020) 100007. https://doi.org/10.1016/j.ijft.2019.100007.

[7] P. Nunez, Sustainable Spent Pot Line Management Guidance, Miner. Met. Mater. Ser. (2020) 1225–1230. https://doi.org/10.1007/978-3-030-36408-3_168.

[8] D.F. Lisbona, C. Somerfield, K.M. Steel, Leaching of spent pot-lining with aluminium nitrate and nitric acid: Effect of reaction conditions and thermodynamic modelling of solution speciation, Hydrometallurgy. 134–135 (2013) 132–143. https://doi.org/10.1016/j.hydromet.2013.02.011.

[9] E.M. Foundation, Towards a Circular Economy: Business Rationale for an Accelerated Transition, Ellen MacArthur Found. (2015) 20.

[10] T.J. Robshaw, K. Bonser, G. Coxhill, R. Dawson, M.D. Ogden, Development of a Combined Leaching and Ion-Exchange System for Valorisation of Spent Potlining Waste, Waste and Biomass Valorization. (2020). https://doi.org/10.1007/s12649-020-00954-1.

[11] W. Xianxi, Z. Weidong, L. Kunlin, W. Song, Alternative Applications of SPL: Testing Ideas Through Experiments and Mathematical Modeling Dawei, Miner. Met. Mater. Soc. (2017) 1357–1364. https://doi.org/10.1007/978-3-319-51541-0.

[12] Z.N. Shi, W. Li, X.W. Hu, B.J. Ren, B.L. Gao, Z.W. Wang, Recovery of carbon and cryolite from spent pot lining of aluminium reduction cells by chemical leaching, Trans.

Nonferrous Met. Soc. China (English Ed. 22 (2012) 222–227. https://doi.org/10.1016/S1003-6326(11)61164-3.

[13] R.P. Pawlek, SPL: An update, Miner. Met. Mater. Ser. Part F4 (2018) 671–674. https://doi.org/10.1007/978-3-319-72284-9_86.

[14] X. Wang, Q. Ge, Separation and recovery of NaF from fluorine containing solution by the common ion effect of Na+, Heliyon. 4 (2018) 1–8. https://doi.org/10.1016/j.heliyon.2018.e01029.

[15] D.F. Lisbona, C. Somerfield, K.M. Steel, Leaching of spent pot-lining with aluminum anodizing wastewaters: Fluoride extraction and thermodynamic modeling of aqueous speciation, Ind. Eng. Chem. Res. 51 (2012) 8366–8377. https://doi.org/10.1021/ie3006353.

[16] European Commission, Study on the review of the list of Critical Raw Materials - Critical Raw Materials Factsheets, 2017. https://doi.org/10.2873/876644.

[17] O. Tkacheva, A. Dedyukhin, A. Redkin, Y. Zaikov, The calcium fluoride effect on properties of cryolite melts feasible for low-temperature production of aluminum and its alloys, AIP Conf. Proc. 1858 (2017) 1–6. https://doi.org/10.1063/1.4989946.

[18] D.F. Lisbona, C. Somerfield, K.M. Steel, Treatment of spent pot-lining with aluminum anodizing wastewaters: Selective precipitation of aluminum and fluoride as an aluminum hydroxyfluoride hydrate product, Ind. Eng. Chem. Res. 51 (2012) 12712–12722. https://doi.org/10.1021/ie3013506.

[19] U. Ntuk, S. Tait, E.T. White, K.M. Steel, The precipitation and solubility of aluminium hydroxyfluoride hydrate between 30 and 70 °c, Hydrometallurgy. 155 (2015) 79–87. https://doi.org/10.1016/j.hydromet.2015.04.010.

[20] G. Zhang, G. Sun, J. Liu, F. Evrendilek, M. Buyukada, W. Xie, Thermal behaviors of fluorine during (co-)incinerations of spent potlining and red mud: Transformation, retention, leaching and thermodynamic modeling analyses, Chemosphere. 249 (2020) 126204. https://doi.org/10.1016/j.chemosphere.2020.126204.

[21] C.Y. Tai, P.C. Chen, T.M. Tsao, Growth kinetics of CaF2 in a pH-stat fluidized-bed crystallizer, J. Cryst. Growth. 290 (2006) 576–584. https://doi.org/10.1016/j.jcrysgro.2006.02.036.

[22] T. Itakura, R. Sasai, H. Itoh, A novel recovery method for treating wastewater containing fluoride and fluoroboric acid, Bull. Chem. Soc. Jpn. 79 (2006) 1303–1307. https://doi.org/10.1246/bcsj.79.1303.

[23] S.K. Jha, R.K. Singh, T. Damodaran, V.K. Mishra, D.K. Sharma, D. Rai, Fluoride in groundwater: Toxicological exposure and remedies, J. Toxicol. Environ. Heal. - Part B Crit. Rev. 16 (2013) 52–66. https://doi.org/10.1080/10937404.2013.769420.

[24] T.J. Robshaw, R. Dawson, K. Bonser, M.D. Ogden, Towards the implementation of an ion-exchange system for recovery of fluoride commodity chemicals. Kinetic and dynamic studies, Chem. Eng. J. 367 (2019) 149–159. https://doi.org/10.1016/j.cej.2019.02.135.

[25] Fluoride Removal from Industrial Wastewater | Saltworks Technologies, (n.d.). https://www.saltworkstech.com/articles/fluoride-removal-from-industrial-wastewater-using-advanced-chemical-precipitation-and-filtration/ (accessed June 24, 2020).

[26] D. Erdemir, A.Y. Lee, A.S. Myerson, Nucleation of crystals from solution: Classical and two-step models, Acc. Chem. Res. 42 (2009) 621–629. https://doi.org/10.1021/ar800217x.

[27] N.T.K. Thanh, N. Maclean, S. Mahiddine, Mechanisms of nucleation and growth of nanoparticles in solution, Chem. Rev. 114 (2014) 7610–7630. https://doi.org/10.1021/cr400544s.

[28] P.H. Karpiński, J. Bałdyga, Precipitation Processes, 2019. https://doi.org/10.1017/9781139026949.008.

[29] C. Lin, A. Chen, J. Tsai, S. Wei, E Ndoscopic R Emoval of F Oreign, 23 (2007) 745–753.

[30] M. Morita, G. Granata, C. Tokoro, Recovery of calcium fluoride from highly contaminated fluoric/hexafluorosilicic acid wastewater, Mater. Trans. 59 (2018) 290–296. https://doi.org/10.2320/matertrans.M-M2017850.

[31] G. El, Fases sólidas en los materiales . Formación de la, (n.d.) 43–47.

[32] A. Roine, K. Anttila, E - pH (Pourbaix) Diagrams and Reaction Equations Module, Outotec. 1 (2018).

[33] J. R. Davis, Corrosion: Understanding the Basics, ASM International, 2000.

[34] B.C. Smith, Fundamentals of Fourier Transform Infrared Spectroscopy, 2nd Editio, 2011. https://doi.org/https://doi.org/10.1201/b10777.

[35] C. Outline, Methods for Assessing Surface Cleanliness, 2019. https://doi.org/10.1016/b978-0-12-816081-7.00003-6.

[36] L. Zeng, Z. Li, Solubility and modeling of sodium aluminosilicate in NaOH-NaAl(OH) 4 solutions and its application to desilication, Ind. Eng. Chem. Res. 51 (2012) 15193–15206. https://doi.org/10.1021/ie301590r.

[37] K.H. Gayer, L.C. Thompson, O.T. Zajicek, the Solubility of Aluminum Hydroxide in Acidic and, 36 (1968) 0–3.

[38] H.A. Craddock, Oilfield Chemistry and its Environmental Impact, 2018.

[39] J.A. Tossell, Theoretical studies on aluminate and sodium aluminate species in models for aqueous solution: A1(OH)3, Al(OH)4-, and NaAl(OH)4, Am. Mineral. 84 (1999) 1641–1649. https://doi.org/10.2138/am-1999-1019.

[40] aqion - Online pH Calculator, (n.d.). http://www.aqion.onl/reacs/new/ (accessed May 15, 2020).

[41] M.M. Emamjomeh, M. Sivakumar, A.S. Varyani, Analysis and the understanding of fluoride removal mechanisms by an electrocoagulation/flotation (ECF) process, Desalination. 275 (2011) 102–106. https://doi.org/10.1016/j.desal.2011.02.032.

[42] R.J. Moolenaar, J.C. Evans, L.D. McKeever, The structure of the aluminate ion in solutions at high pH, J. Phys. Chem. 74 (1970) 3629–3636. https://doi.org/10.1021/j100714a014.

[43] D.J. Wesolowski, Aluminum speciation and equilibria in aqueous solution: I. The solubility of gibbsite in the system Na-K-Cl-OH-Al(OH)4 from 0 to 100°C, Geochim. Cosmochim. Acta. 56 (1992) 1065–1091. https://doi.org/10.1016/0016-7037(92)90047-M.

[44] M. Sivakumar, M.M. Emamjomeh, Electrochemical method for fluoride removal: Measurement, Speciation and Mechanisms Electrochemical method for fluoride removal: Measurement, Speciation, and Mechanisms, Environ. Postgr. Conf. Environ. Chang. Mak. It Happen. 61 (2005) 1–8. http://ro.uow.edu.au/engpapers/1661.

[45] S. Schrödle, E. Königsberger, P.M. May, G. Hefter, Heat capacities of aqueous sodium hydroxide/aluminate mixtures and prediction of the solubility constant of boehmite up to 300 °C, Geochim. Cosmochim. Acta. 74 (2010) 2368–2379. https://doi.org/10.1016/j.gca.2010.01.002.

[46] PubChem, (n.d.). https://pubchem.ncbi.nlm.nih.gov/ (accessed July 6, 2020).

[47] Chemistry-Reference, n.d. http://chemistry-reference.com/.

[48] M. Markovic, S. Takagi, L.C. Chow, S. Frukhtbeyn, Calcium fluoride precipitation and deposition from 12 mmol/L fluoride solutions with different calcium addition rates, J. Res. Natl. Inst. Stand. Technol. 114 (2009) 293–301. https://doi.org/10.6028/jres.114.021.

[49] J. Coates, Interpretation of Infrared Spectra, A Practical Approach, Encycl. Anal. Chem. (2006) 1–23. https://doi.org/10.1002/9780470027318.a5606.

A. APPENDIX A

All the proposed species considered in the simulation are shown:

$$NaF_{(a)} = Na^+ + F^-$$

$$NaAl(OH)_{4\,(a)} = Na^+ + Al^{3+} + OH^-$$

$$NaOH = NaOH_{(a)} = Na^+ + OH^-$$

$$NaAlF_{4(g)} = Na^+ + Al^{3+} + F^-$$

$$AlF_3 = AlF_{3(a)} = AlF_2^+ + F^- = AlF^{2+} + F^- = AlF_4^- + Al^{3+} = AlF_5^{2-} + Al^{3+} = AlF_6^{3-} + Al^{3+} = Al^{3+} + F^-$$

$$Al(OH)_3 = Al(OH)_{3(a)} = Al(OH)_2^+ + OH^- = AlOH^{2+} + OH^- = Al(OH)_4^- + Al^{3+} = Al^{+3} + OH^-$$

$$CaCl_{2(a)} = CaCl^+ + Cl^- = Ca^{2+} + Cl^-$$

$$NaCl = NaCl_{(a)} = Na^+ + Cl^-$$

$$Ca(OH)_2 = Ca(OH)_{2(ia)} = CaOH^+ + OH^- = Ca^{2+} + OH^-$$

$$NaAlCl_4 = Na^+ + Al^{3+} + Cl^-$$

$$AlCl_3 = AlCl_{3(a)} = Al^{3+} + Cl^-$$

$$CaF_2 = CaF_{2(ia)} = Ca^{2+} + F^-$$

$$Al_2O_3$$

$$Cl_{2(g)}$$

$$CaO$$

$$H_2O$$

$$Na_2O$$

$$CaCO_{3(a)} = Ca^{2+} + CO_3^{2-}$$

$$Na_2CO_3 = Na_2CO_{3(ia)} = Na^{2+} + CO_3^{2-} = NaCO_3^- + Na^+$$

$$NaAlCO_3(OH)_2$$

$$Al_2(CO_3)_{3(a)} = Al^{3+} + CO_3^{2+}$$

B. APPENDIX B

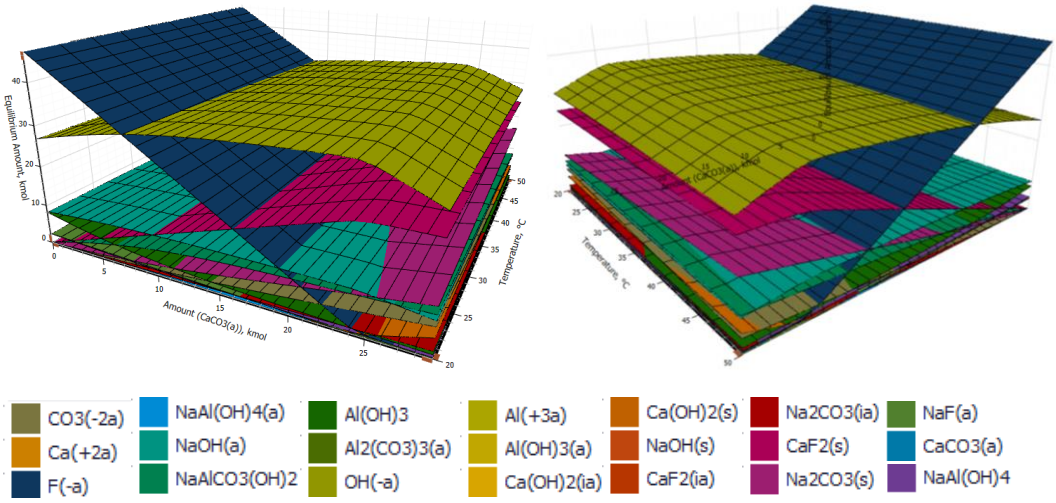

Figure 30 Equilibrium amount evolution of each component according to the added amount of $CaCO_3$ and temperature.

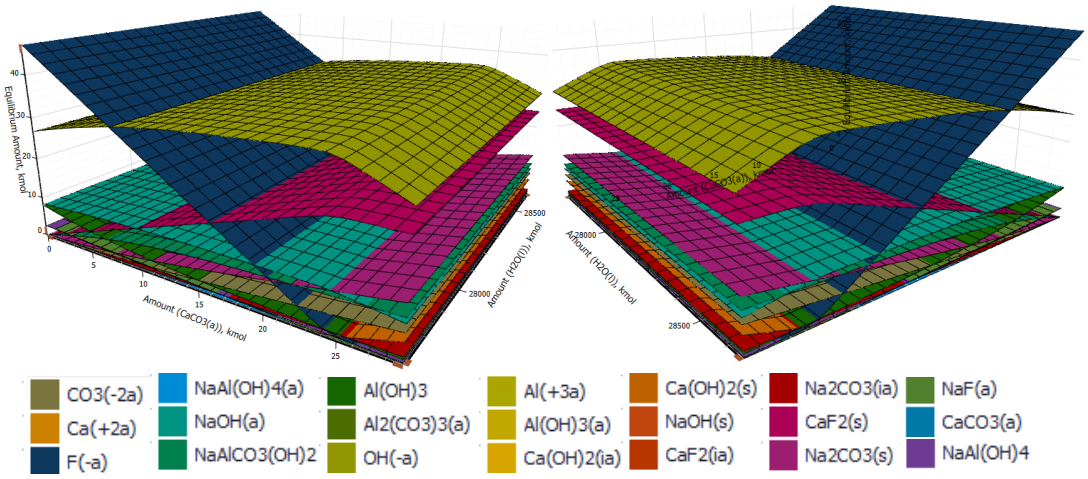

Figure 31 Equilibrium amount evolution of each component according to the added amount of $CaCO_3$ and water.

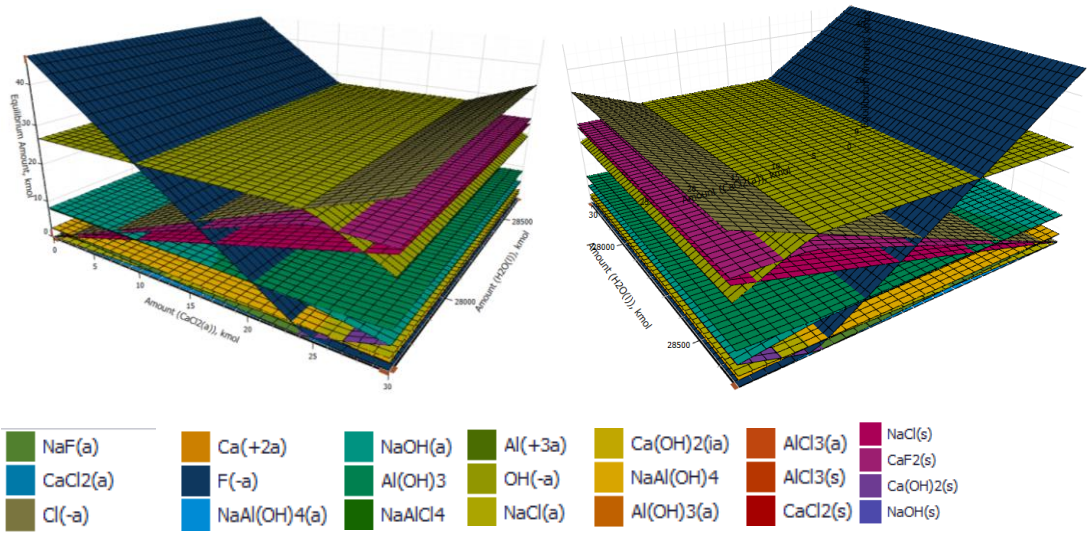

Figure 32 Equilibrium amount evolution of each component according to the added amount of $CaCl_2$ and water.

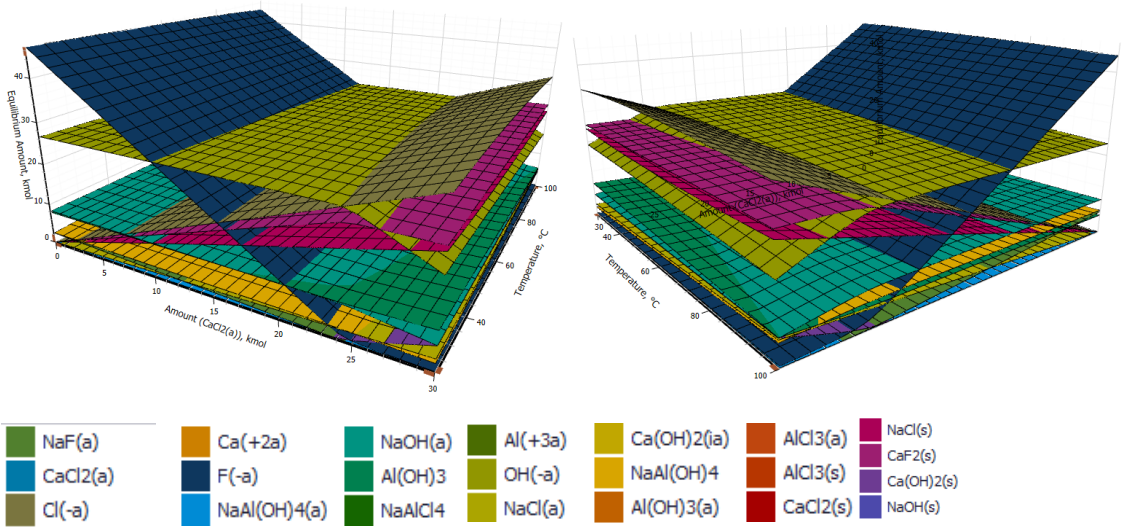

Figure 33 Equilibrium amount evolution of each component according to the added amount of $CaCl_2$ and temperature.

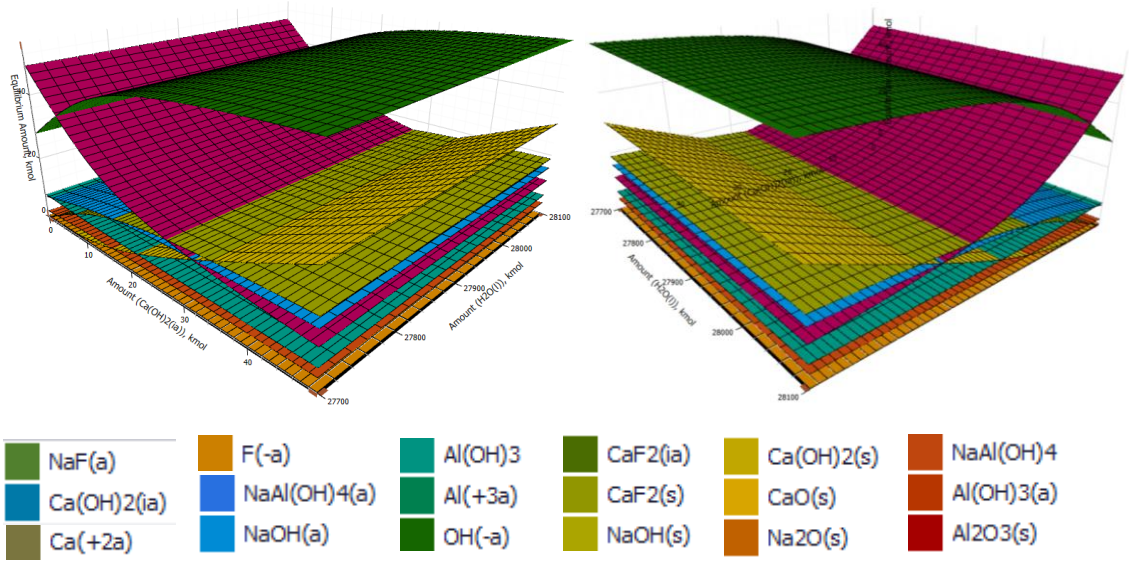

Figure 34 Equilibrium amount evolution of each component according to the added amount of $Ca(OH)_2$ and water.

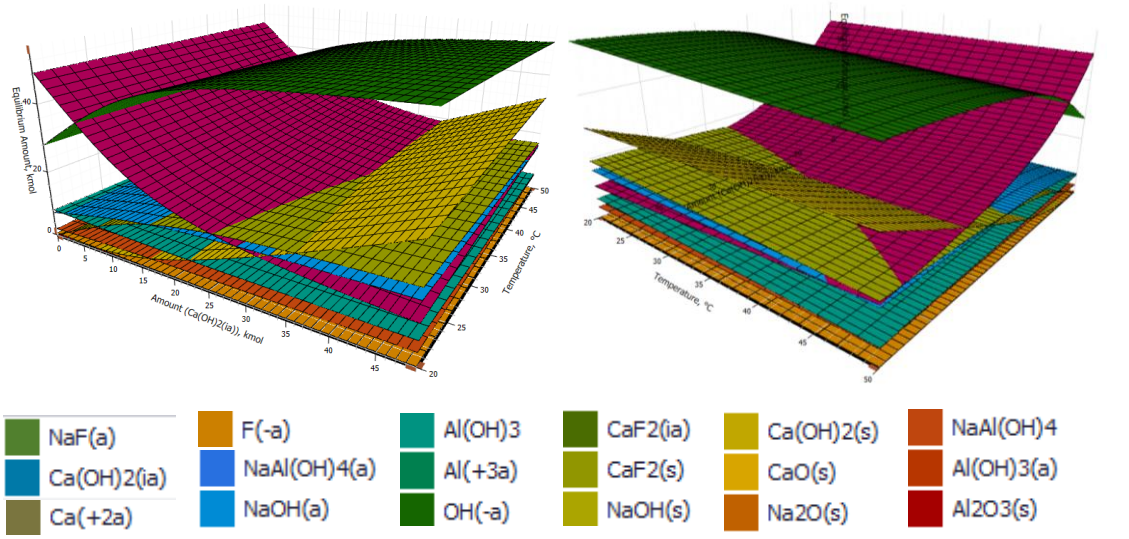

Figure 35 Equilibrium amount evolution of each component according to the added amount of $Ca(OH)_2$ and temperature.

C. APPENDIX C

	kmol	*kmol/h*	*mmol/L*	*pH*	*pOH*	*[OH-]*	
NaF(a)	1.49E-02	1.49E-06	3.03E-02	7.01	6.99	1.02E-07	
CaCO3(a)	8.24E-04	8.24E-08	1.67E-03	8.23	5.77	1.70E-06	
NaAl(OH)4(a)	6.40E-03	6.40E-07	1.30E-02	7.51	6.49	3.24E-07	
NaOH(a)	8.85E+00	8.85E-04	17.98	12.19	1.81	1.55E-02	
Al2(CO3)3(a)	6.70E-69	6.70E-73	1.36E-68				
Al(OH)3(a)	1.55E-09	1.55E-13	3.15E-09	7	7.00	1.00E-07	
Ca(OH)2(ia)	2.53E-07	2.53E-11	5.14E-07	7	7.00	1.00E-07	
CaF2(ia)	2.41E-12	2.41E-16	4.89E-12				
Na2CO3(ia)	1.32E+00	1.32E-04	2.68E+00	10.73	3.27	5.37E-04	
						1.60E-02	**[OH-] total**
						1.80	POH
						12.20	**PH**

Table 24 Data obtained for the calculation of the pH of the solution ($CaCO_3$)

	kmol	*kmol/h*	*mmol/L*	*pH*	*pOH*	*[OH-]*	
NaF(a)	0.0115	1.15E-06	2.33E-02	7.01	6.99	1.02E-07	
CaCl2(a)	6.75E-08	6.75E-12	1.37E-07	7	7	1.00E-07	
NaAl(OH)4(a)	0.0380	3.80E-06	7.73E-02	7.84	6.16	6.92E-07	
NaOH(a)	6.7442	6.74E-04	13.70	12.08	1.92	1.20E-02	
NaCl(a)	2.4809	2.48E-04	5.04	7	7	1.00E-07	
Ca(OH)2(ia)	2.49E-07	2.49E-11	5.05E-07	7	7	1.00E-07	
Al(OH)3(a)	1.21E-08	1.21E-12	2.46E-08	7	7	1.00E-07	
AlCl3(a)	1.46E-33	1.46E-37	2.96E-33				
						1.20E-02	**[OH-]**
						1.92	POH
						12.08	**PH**

Table 25 Data obtained for the calculation of the pH of the solution ($CaCl_2$)

	kmol	*kmol/h*	*mmol/L*	*pH*	*pOH*	*[OH-]*	
NaF(a)	0.0077	7.69E-07	1.56E-02	7.01	6.99	1.02E-07	
Ca(OH)2(ia)	2.16E-06	2.16E-10	4.40E-06	7	7	1.00E-07	
NaAl(OH)4(a)	0.0680	6.80E-06	1.38E-01	7.96	6.04	9.12E-07	
NaOH(a)	15.5472	1.55E-03	31.58	12.42	1.58	2.63E-02	
CaF2(ia)	1.78E-12	1.78E-16	3.61E-12				
Al(OH)3(a)	9.42E-09	9.42E-13	1.91E-08	7	7	1.00E-07	
						2.63E-02	**[OH-]**
						1.58	POH
						12.42	**PH**

Table 26 Data obtained for the calculation of the pH of the solution ($Ca(OH)_2$)

DEPARTMENT OF CHEMISTRY AND
CHEMICAL ENGINEERING
CHALMERS UNIVERSITY OF TECHNOLOGY
Gothenburg, Sweden

CHALMERS
UNIVERSITY OF TECHNOLOGY